energy partners

DOE/GO/10340--T1

Integrated Renewable Hydrogen Utility System (IRHUS)

Technical Analysis and Plan Development

Phase I

Final Report

Reporting period: April 1 – December 31, 1999

contract: DE-FC36-98GO10340

Submitted to:

U.S. Department of Energy

Prepared by:

Energy Partners, L.C.
1501 Northpoint Parkway, #102
West Palm Beach, FL 33407

Program Manager:
Dr. Frano Barbir

March 1999

DISCLAIMER

Integrated Renewable Hydrogen Utility System (IRHUS)
Technical Analysis and Plan Development
Final Report

TABLE OF CONTENTS

Business plan is prepared as a separate volume

Participants

This report is the result of research and engineering efforts of the following participants:

Energy Partners, L.C.
1501 Northpoint Parkway, #102
West Palm Beach, FL 33407

Frano Barbir, Program Manager
Yan Ngu

Treadwell, Corporation
P.O. Box 458, 341 Railroad St.,
Thomaston, CT 06787

Jonathan Hoadley

Trace Engineering
5916 195th Northeast
Arlington, WA 98233

Cristopher Freitas

Gee&Jenson Engineering
One Harvard Circle
West Palm Beach, FL 33409

James Khalil
Deveren Peterkin

Florida Solar Energy Center
1679 Clearlake Road
Cocoa, FL 32922

Philip Fairey
Nazim Muradov
Eric Martin

Perry Foundation
1501 Northpoint Parkway, #101
West Palm Beach, FL 33407

C. Reneé Cooper

1. Background

Energy Partners is a developer and manufacturer of PEM fuel cells and fuel cell systems. To date we have built several fuel cell stacks and systems up to 20 kW power output. The fuel cell stacks and systems built by Energy Partners are pre-production prototypes. Fuel cell technology is very close to commercialization. However, for commercialization one must have a market. The fuel cells have a tremendous market potential in:

- automotive applications;
- marine applications;
- space applications;
- stationary power generation; and
- military applications.

Each market segment has its own requirements including the cost at which it would be possible to penetrate the market. Although most of the PEM fuel cell development efforts are directed toward automotive applications, earlier market penetration may be feasible in other market segments. Energy Partners in cooperation with utility companies has identified market opportunities in residential power supplies rated at 2-10 kW, off-grid or grid integrated. The biggest obstacle in reaching this market is fuel availability. PEM fuel cells run on relatively pure hydrogen, which is not readily available. Energy Partners' approach is to use natural gas and reform it before using it in fuel cells. Each fuel cell unit therefore must be equipped with a fuel processor. The first prototype of an integrated natural gas fueled fuel cell system has been completed and is currently being tested in Energy Partners laboratories. A pre-production prototype (or prototypes) will be developed next and tested in real-life application.

Another option to provide hydrogen fuel for PEM fuel cells would be to use renewable energy sources for hydrogen generation. Such a system would increase potential markets for stationary fuel cell power systems since it would not have to be tied to either the power grid or natural gas supply line. It may be used to provide both electricity and fuel in remote locations and on islands. Since such a system would generate absolutely zero emissions it may be suitable for ecologically sensitive areas, such as national parks. In addition, the system may also be used for power storage and load leveling for renewable power plants, such as solar, wind, hydro-electric or geothermal power plants.

2. Description of the Integrated Renewable Hydrogen Power System

The proposed integrated hydrogen energy system consists of an electrolyzer, hydrogen and oxygen storage systems, fuel cell system and controller/power conditioning unit (Figure 1). The system must be connected with a renewable power source, such as a photovoltaic array, solar thermal power plant, wind turbine, ocean current turbine-generator, small hydro power plant, or geothermal power plant. The system uses excess electrical power, during periods when power generation exceeds power demand, to produce hydrogen and oxygen. The electrolyzer will be a proton exchange membrane type capable of operating at high pressure (800-1000 psig), developed and manufactured by Treadwell Corp. Hydrogen and oxygen produced will be stored in pressure tanks at pressures up to the electrolyzer operating pressure (800-1000 psig), so that

no additional compression will be needed. During periods when the power demand exceeds power production from renewable energy sources, power will be produced by the fuel cell. The fuel cell will also be of the PEM type, developed and manufactured by Energy Partners. The fuel cell may operate with either pure oxygen (which will be available from the electrolysis process) or air at an operating pressure of up to 50 psig (4.5 bar), and operating temperature up to 80°C.

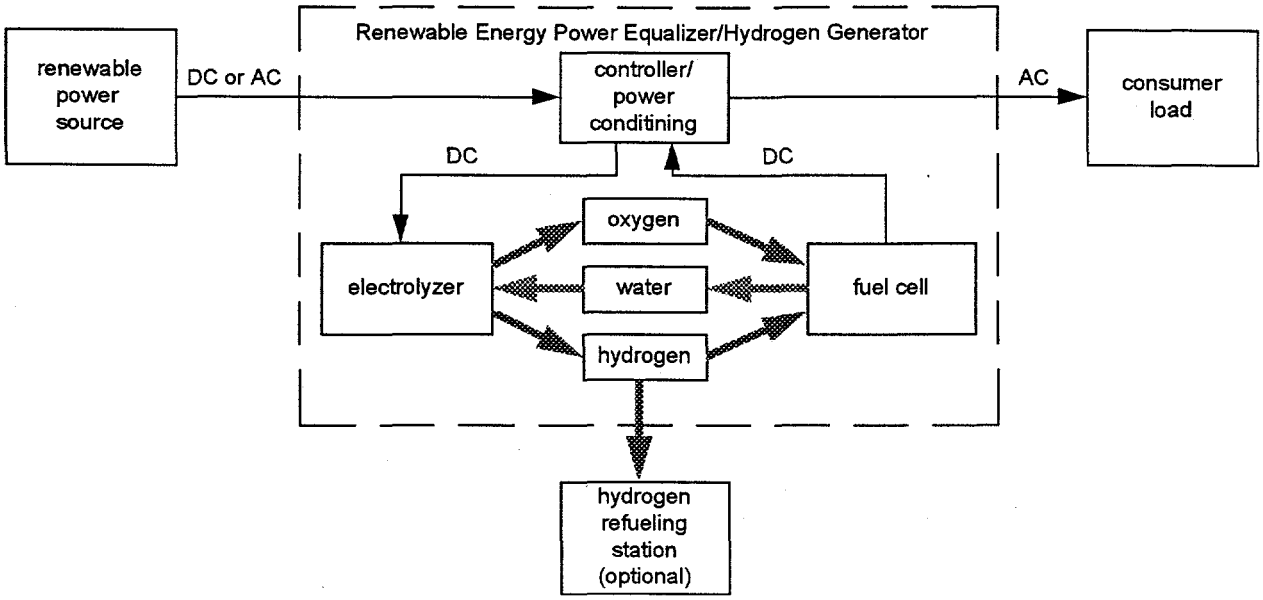

Figure 2.1 Proposed Integrated Renewable Hydrogen Fuel Cell Power System

The supporting systems include handling of the produced/reactant gases and water, heat management system, and controls and power conditioning. Handling of the product/reactant gases includes the control of flow rate, pressure, temperature and humidity. Product water from the fuel cell is used as a feed for the electrolyzer, as well as a cooling medium. The heat management system serves both the electrolyzer and fuel cell. This includes a tank, pump, filter(s), heat exchanger(s), piping, and controls.

The controller/power conditioning unit (CPCU) has a crucial role in operation of the system. The main role is to manage the output of the renewable power source in order to provide a regulated supply of AC current to the consumer load at all times. The renewable power source may generate either DC (photovoltaic array) or AC (wind, hydro or geothermal power plant). In the former case the CPCU will have to be designed to regulate the voltage of the renewable power source and match it to the electrolyzer operating voltage, and to regulate the renewable power source and fuel cell DC and convert it to AC to be delivered to the consumer load. In the latter case the CPCU will have to be designed to forward AC from the renewable power source to the consumer. Excess AC from the renewable power source will be converted into DC with voltage matching that of the electrolyzer. The fuel cell power output (DC) will be converted into usable AC and delivered to the consumer load. The CPCU will also handle the control and monitoring of the fuel cell and electrolyzer operational envelopes.

3. Technology Assessment

3.1 Fuel cells

In the last decade a remarkable progress has been made in the performance of PEM fuel cells, i.e. power density, efficiency, and cost reduction. These advances, as well as the inherent property of being clean power sources, have made PEM fuels an interesting alternative power generator. Particularly for transportation purposes, PEM fuel cells may be the only solution that can meet high efficiency and ultra-low emissions goals without impacting customer expectations for cost or performance.

Energy Partners has been working on the development of PEM fuel cells since 1989. Major accomplishments in this period include:

- fuel cell powered commercial submarine (PC1401) completed in 1989
- fuel cell powered passenger car, EP GreenCar, completed in 1993
- 2.5-4 kW bench top laboratory fuel cell and supporting system delivered to the Australian Ministry of Defense, Material Research Laboratory, in 1992. A similar system delivered to Belgian research organization VITO in 1993.
- Genesis, hydrogen/oxygen fuel cell powered transporter, completed in 1995, and demonstrated in Atlanta during the Olympic Games, 1996.
- 10 kW fuel cell stack delivered to Ford Motor Company in 1996
- several fuel cell stacks ranging from 2-10 kW delivered to customers in USA, Spain and Germany,
- three John Deere Gators equipped with 10 kW fuel cell power system; two delivered to Palm Springs Airport in June 1997 for testing and demonstration
- new generation advanced stack (NG2000) developed in 1998; 20 kW stacks (pressurized H_2/air) delivered to Virginia Tech (Figure 3.1) and Texas Tech for Future Car Challenge; several smaller stacks (3-5 kW) delivered to customers.

Energy Partners has significantly advanced state-of-the-art PEM fuel cell stack technology. Multi-kilowatt fuel cell stacks (up to 20 kW) have been built, tested, and delivered to customers (Figure 3.1). Power density of >0.7 W/cm^2 has been demonstrated in full scale stacks (20 kW) with 300 cm^2 active area operating with pressurized H_2 and air. Table 3.1 shows the technical characteristics of the Energy Partners' state-of-the-art fuel cell stacks. Figure 3.2 shows the polarization curve of a 20 kW stack.

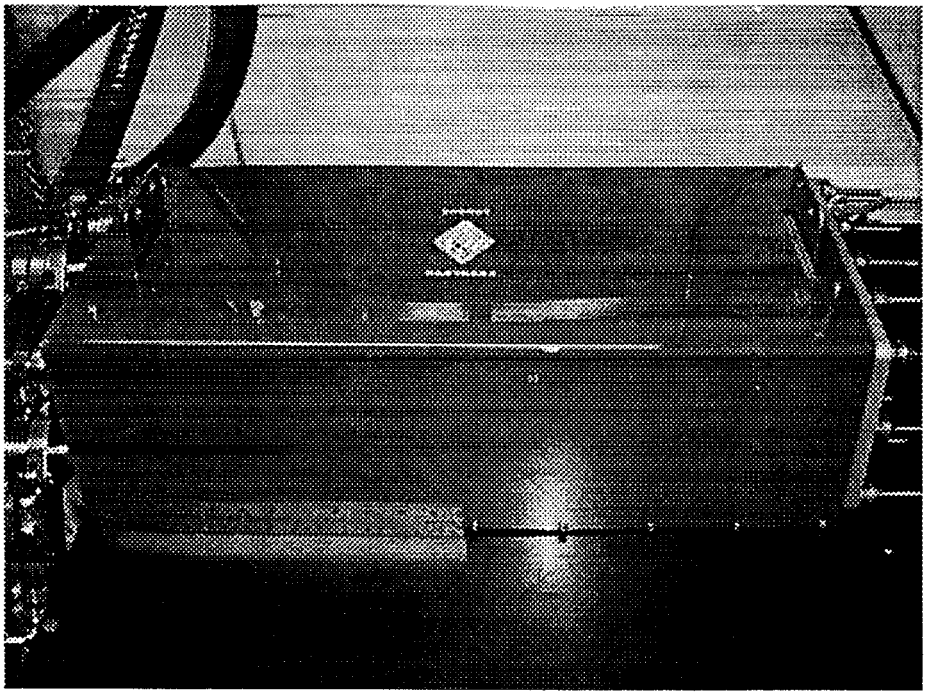

Figure 3.1 Energy Partners 20 kW stack (NG2000)

Table 3.1 Characteristics of Energy Partners state-of-the-art fuel cell stacks (NG2000)

Nominal power output	up to 20 kW
Cell voltage at nominal power	0.6 V
Number of cells	up to 110
Cell active area	292 cm^2
Maximum power density	0.7 W/cm^2
Platinum loading	0.35 mg/cm^2 (total)
Reactants	H_2/air
Operating pressure (inlet)	up to 3 bar (30 psig)
Operating temperature	60-65°C
Dimensions WxHxL	29x17x68 (110-cell stack)
Weight	65 kg (110-cell stack)
Gravimetric power density	0.34 kW/kg
Volumetric power density	0.66 kW/l

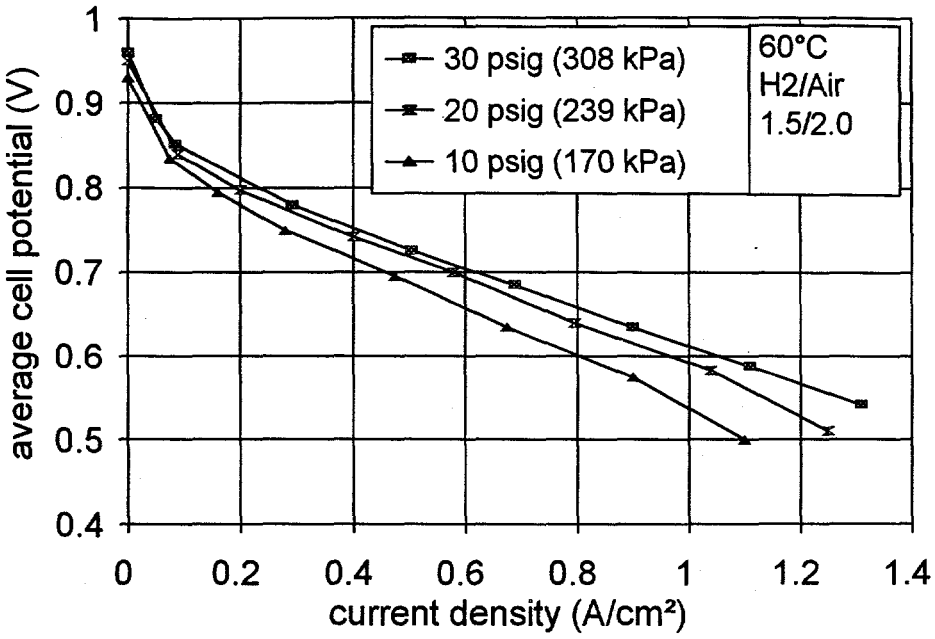

Figure 3.2 Polarization curves of a 20 kW stack (NG2000)

Although, Energy Partners could be manufacturing the NG2000 stacks in relatively large series, there is no large market for such stacks, primarily because hydrogen as fuel is not readily available. In order to commercialize its fuel cell technology, Energy Partners has started development of natural gas fueled stationary power systems in a 2.5-7.5 kW range. These systems include natural gas fuel processors and reformate tolerant fuel cell stacks (NG2000R).

Energy Partners has produced more than 100 multi-kW stacks for internal projects and sales to the customers. The stacks are made from the purchased and manufactured components (see Table 3.2). The only major components that are purchased are the membrane/electrode assemblies and gas diffusers. All other stack components are manufactured by Energy Partners. This includes the bi-polar collector/separator plates which are produced by a proprietary molding process. Energy Partners is currently working on a process for mass production of bi-polar plates.

Present cost of the Energy Partners fuel cell stacks is high because the stacks are produced as prototypes on a one-by-one basis. Figure 3.3 shows the breakdown of current system and stack manufacturing costs. The design and the manufacturing process is suitable for large series production. Table 3.3 shows current and projected manufacturing costs for the fuel cell stack and for the entire fuel cell system. The resulting cost decrease is due to changes in quantities and changes in manufacturing process.

Table 3.2 Fuel cell stack components

part	material	manufacturer/process
membrane	fluorinated polymer	W.L. Gore, DuPont, Asahi
electrode	Pt, carbon, Teflon	W.L. Gore, Johnson Matthey, E-TEK, 3M
gas diffusion layer	carbon cloth or paper	E-TEK, Spectracorp
bi-polar plates	graphite/polymer	molding
bus plates	copper	machining, gold plating
end plates	stainless steel, aluminum, composite	machining, casting

Table 3.3 Energy Partners present and future fuel cell manufacturing costs

	current cost prototype level (several per year)	future cost manufacturing level (1,000 units/yr)	future cost mass production level (50,000 units/yr)
Fuel cell stack			
membrane/electrodes	0.90/cm^2	0.19 /cm^2	0.009 /cm^2
gas diffusers	1.01/cm^2	0.21 /cm^2	0.010 /cm^2
bipolar plates	0.46/cm^2	0.10 /cm^2	0.013 /cm^2
other parts	0.26/cm^2	0.05 /cm^2	0.003 /cm^2
assembly	0.32/cm^2 + 8,566/stk	0.07/cm^2 + 1700/stk	0.003/cm^2 +100/stk
total stack	**2.95/cm^2 + 8,566/stk**	**0.62/cm^2 + 1,700/stk**	**0.038/cm^2 + 100/stk**
	6,757/kW	**1,410/kW**	**86/kW**
Fuel cell system			
parts	7,455/kW	1,000/kW	385/kW
assembly	5,016/kW	500/kW	100/kW
total system	**19,228/kW**	**2,910/kW**	**571/kW**

Notes:

- costs include overhead, G&A, and profit
- based on current design, 300 cm^2 0.5 W/cm^2
- based on a 10 kW system

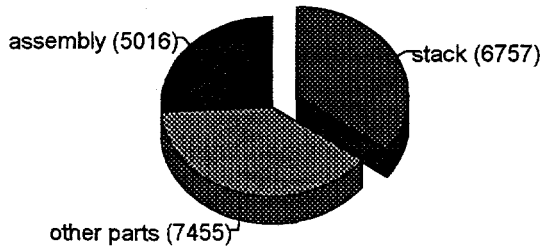

Figure 3.3a System cost (current)

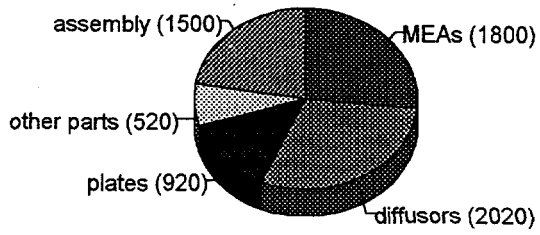

Figure 3.3b Stack cost (current)

3.2 Electrolyzer

Three high pressure Proton Exchange Membrane (PEM) based electrolyzers producing 21 MPa (3,000 psig) hydrogen and oxygen gas were recently manufactured by Treadwell Corporation in partnership with Giner, Inc. These PEM electrolyzers (Oxygen Generating Plant - Figure 1) are used to produce breathing oxygen for the crews of the SEAWOLF Class of U.S. Navy Nuclear Submarines. An expensive pressure dome control system was required to produce the hydrogen and oxygen gas at this extremely high pressure.

Giner was responsible for the manufacturing of the stack components (over five thousand individual cell stack components) for six, 100-cell Oxygen Generating Plant (OGP) electrolyzer stacks (Figure 3.5). This consisted of fabricating catalysts, membrane-electrode assemblies, screen assemblies, separators, pressure pads and gaskets. Treadwell inspected and assembled the components into 100-cell units. Treadwell manufactured and qualified the OGP systems.

Treadwell and Giner now have teamed to develop an advanced, low-cost, PEM electrolyzer capable producing oxygen and hydrogen at pressures up to 6.9 MPa (1000 psi) while operating efficiently at high current densities of up to two thousand mA/cm^2 (amps/sq. ft.). Life testing of both single and 4-cell stacks of this commercial cell design has demonstrated highly stable operation throughout a thirty thousand-hour life endurance test. Cell voltage degradation rate averages approximately 3×10^{-6} volts/hr. Life tests are continuing. The advanced stacks can operate at a 1000-psi pressure differential across the membrane and electrode assemblies, as well as to the outside ambient. In this design there is no pressure dome required. The stacks operate at 55°C (130°F) with the hydrogen side at approximately 6.9 MPa (1000 psi) and oxygen at ambient pressure. Cell active area is approximately 280 cm^2 (0.3 square feet).

Typical cell performance is shown in Figure 3.6 for an electrolysis cell containing Nafion 1100 and 1200 equivalent weight (EW) membranes, Nafion - 110 (10 mil, 1100 EW), 117 (7 mil, 1100 EW), and 120 (10 mil and 1200 EW). The Nafion 120 and 110 cell stacks are designed for the military application. For this commercial application we plan to utilize the Nafion 117 membrane, which is the lowest cost and exhibits the highest voltage efficiency. Expected cell voltage at normal operating conditions of 1.5 A/cm^2 (1400 A/ft^2), 55°C (130°F) is approximately 1.9 V.

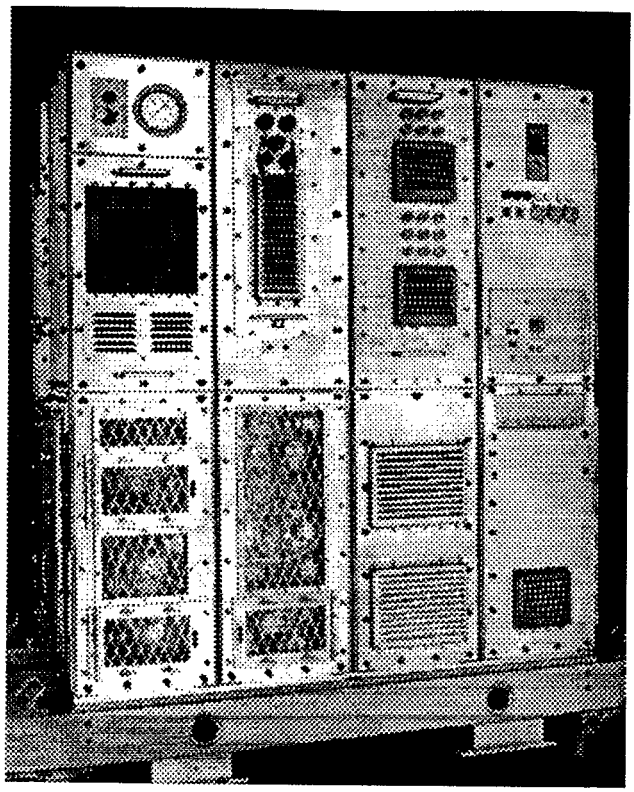

Figure 3.4 Oxygen Generating Plant

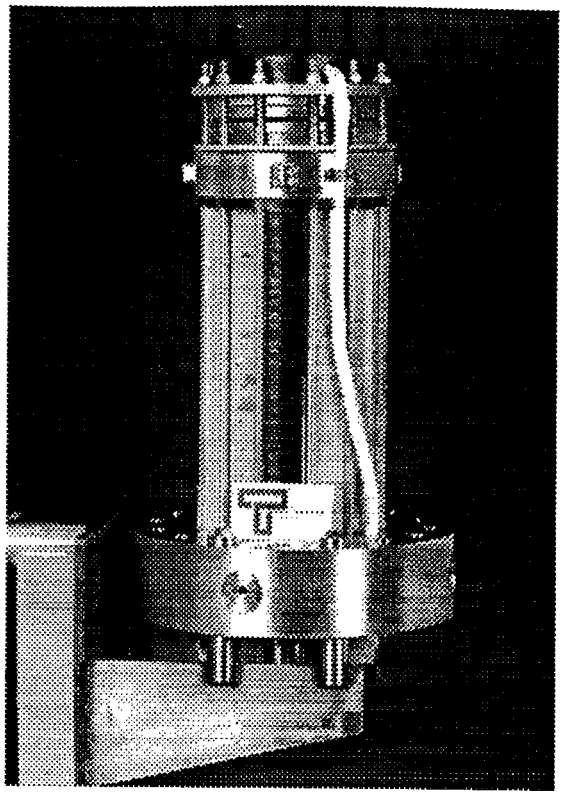

Figure 3.5 Oxygen Generating Plant Electrolyzer Cell Stack

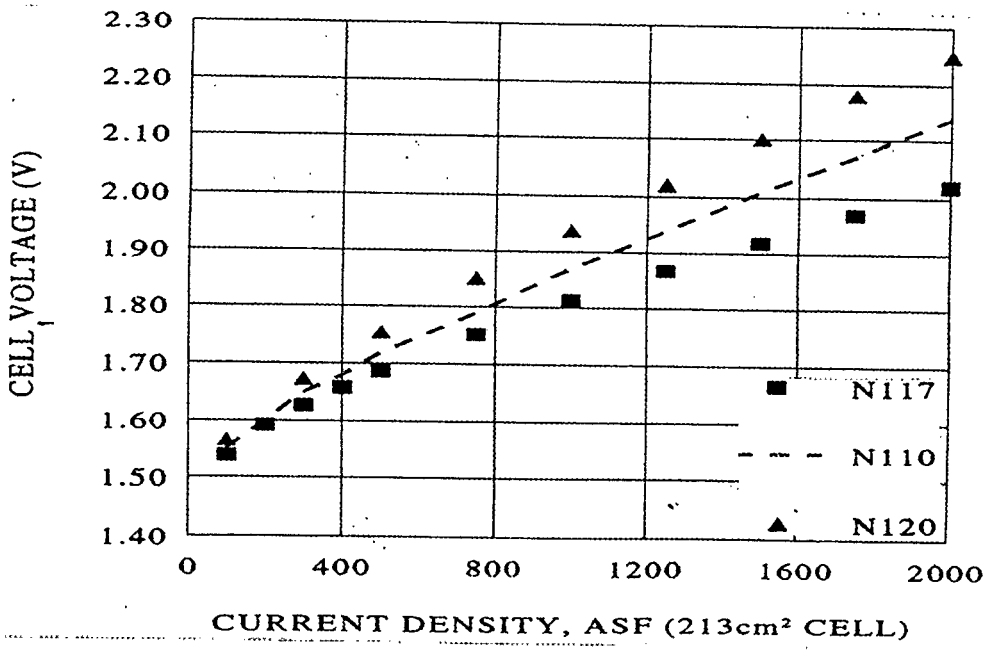

Figure 3.6 Typical Cell Performance for an Electrolysis Cell Containing Nafion 1100 and 1200 Equivalent Weight (EW) Membranes.

We are not aware of any competitive, low-cost PEM or alkaline electrolyzers that have the capability for long life and efficient operation at 6.9 MPa (1000 psi) operating pressure.

Most of the competitive electrolyzer technologies for hydrogen generation are of the low-pressure alkaline type. These electrolyzers have been limited to date, due to low current density (< 500 A/Ft^2) and pressure (≤ 200 psi) generation limitations. Some commercial alkaline electrolytic hydrogen suppliers include Teledyne Corp. (USA), Electrolyzer Corp. (Canada) and DeNora (Italy).

Current PEM electrolyzer systems sold by Hamilton Standard Division, UTC, are prohibitively expensive. Recently, Proton Energy Systems has developed PEM electrolyzer systems; however, operating pressure is limited to relatively low pressure (1.75 MPa, 250 psi) and life and reliability have not been established. Our goal for the proposed high-pressure, PEM electrolyzer is to be lower in price than an equivalent alkaline electrolyzer.

In the area of cost, electrolyzer cell performance plays a major role. The number of cells in a stack of cells affects total unit cost while efficiency of a single cell affects the area required for a given electrical input, resulting in the operating cost for a given size cell. Treadwell and Giner are continuing to develop improved, low-cost catalysts and low contact resistance current collectors, thus improving performance and lowering cost.

The cost estimate for the first, commercial, high pressure hydrogen generator prototype, containing a PEM electrolyzer cell stack consisting of 16 cells of approximately 280 cm^2 (0.3 Ft^2) active area/cell, capable of producing 100 SCFH of 6.9 MPa (1000 psi) hydrogen gas when operated at 1.6 A/cm^2 (1500 A/Ft^2) or 450 amps, is $250,000. The proposed configuration uses typical noble metal electrolyzer catalyst loading (8.6 mg/cm^2 or 8 g/Ft^2 per cell), Nb screens on the oxygen anode side, embossed cell frames, Zr screens on the hydrogen cathode side, and advanced pressure pad design.

Planned cost reductions include:

1. Streamlining the membrane and electrode assembly (MEA) manufacturing (painting or screen printing as is currently practiced in fuel cell processing
2. Lowering noble metal catalyst and current collector costs by at least a factor of 2
3. Quantity procurement of components
4. Use of molded cell frames
5. More automated processing of metallic and polymer components
6. Higher current density stack operation.

It is estimated that with the above changes, production costs could be reduced to under $50,000 per system. Operation at 2.15 A/cm^2 (2000 A/Ft^2) would further reduce the cost, but would also reduce overall energy efficiency.

3.3 Hydrogen storage

Depending on the load and source power profiles and their seasonal variations, a 10 kW integrated renewable hydrogen utility system would need to store between 500 and 2,000 standard cubic meters (40-170 kg) of hydrogen. Hydrogen would be produced at 6.9 MPa (1000 psi). Because of hydrogen's low density its storage always requires relatively large volumes and is associated with either high pressures (thus requiring heavy vessels), or extremely low temperatures, and/or combination with other materials (much heavier than hydrogen itself). Table 3.1 shows achievable storage densities with different types of hydrogen storage. Some novel hydrogen storage method may achieve even higher storage densities, but have yet to be proven in terms of practicality, cost and safety.

Table 3.1 Hydrogen Storage Types and Densities

	kg H_2 /kg	kg H_2/m^3
Large volume storage (10^2 to 10^4 m^3 geometric volume)		
Pressurized gas storage	0.01-0.014	2-16
Metal hydride	0.013-0.015	50-55
Liquid hydrogen	~1	65-69
Stationary small storage (1 to 100 m^3 geometric volume)		
Pressurized gas cylinder	0.012	~15
Metal hydride	0.012-0.02	50-55
Liquid hydrogen tank	0.15-0.50	~65
Vehicle tanks (0.1 to 0.5 m^3 geometric volume)		
Pressurized gas cylinder	0.05	15
Metal hydride	0.012-0.02	50-55
Liquid hydrogen tank	0.09-0.13	50-60

Pressurized gas storage systems

Technically the easiest way to store hydrogen is in pressurized tanks, particularly if hydrogen is already produced at relatively high pressure. A pressure of 1,000 psi (69 bar) does not require any special materials or construction. Cylindrical pressure vessels or tube banks can be used for storage amount up to 2,000-4,000 Nm^3 (165-335 kg) of hydrogen. These storage systems are very heavy and at 69 bars stored hydrogen makes less than 1% of the total weight.

However, for stationary applications weight is not of crucial importance. In cases where mobility of the power system is important, new lightweight composite tanks may be considered (the same

that are being considered for automotive applications). These tanks, even at small sizes (about 0.5 kg hydrogen per tank at 68 bar) can store up to 2% hydrogen by weight. Increasing the storage pressure may increase the storage capacity up to 2-3 times. However, this adds an additional component - a compressor, which not only increases complexity and cost of the system but also reduces the overall efficiency.

Oxygen can be stored in the same type of tanks, although special (but standardized) procedures must be applied for cleaning and degreasing of oxygen tanks, piping and valves. A trade-off study must be conducted to justify oxygen storage, i.e., whether the capital cost, volume and safety aspects of oxygen storage compare with higher capital cost and lower system efficiency of hydrogen/air fuel cells.

Metal hydride storage

Hydrogen can form metal hydrides with some metals and alloys. During the formation of the metal hydride hydrogen molecules are split and hydrogen atoms are inserted in spaces inside the lattice of suitable metals and/or alloys. In such a way an effective storage is created comparable to the density of liquid hydrogen. However, when the mass of the metal or alloy is taken into account then the metal hydride gravimetric storage density is comparable to storage of pressurized hydrogen. The best achievable gravimetric storage density is about 0.07 kg of H_2/kg of metal, for a high temperature hydride such as MgH_2 as shown in Table 3.3. It gives a comparison of some hydriding substances with liquid hydrogen, gaseous hydrogen and gasoline.

During the storage process (charging or absorption) heat is released which must be removed in order to achieve the continuity of the reaction. During the hydrogen release process (discharging or desorption) heat must be supplied to the storage tank.

An advantage of storing hydrogen in hydriding substances is the safety aspect. A serious damage to a hydride tank would not pose fire hazard since hydrogen would remain in the metal structure.

Table 3.3 Hydriding Substances as Hydrogen Storage Media

Medium	Hydrogen Content kg/kg	Hydrogen storage capacity kg/l of vol.	Energy density kJ/kg	Energy density kJ/l of vol.
MgH_2	0.070	0.101	9,933	14,330
Mg_2NiH_4	0.0316	0.081	4,484	11,494
VH_2	0.0207		3,831	
$FeTiH_{1.95}$	0.0175	0.096	2,483	13,620
$TiFe_{0.7}Mn_{0.2}H_{1.9}$	0.0172	0.090	2,440	12,770
$LaNi_5H_{7.0}$	0.0137	0.089	1,944	12,630
$R.E.Ni_5H_{6.5}$	0.0135	0.090	1,915	12,770

Novel hydrogen storage methods

Hydrogen can be physically adsorbed on activated carbon and be "packed" on the surface and inside the carbon structure more densely than if it has been just compressed. Amounts of up to 48 g H_2 per kg of carbon have been reported at 6.0 MPa and 87 K [1]. The adsorption capacity is a function of pressure and temperature, therefore at higher pressures and/or lower temperatures even larger amounts of hydrogen can be adsorbed. For any practical use, relatively low temperatures are needed (<100 K). Since the adsorption is a surface process, the adsorption capacity of hydrogen on activated carbon is largely due to the high surface area of the activated carbon, although there are some other carbon properties which affect the capability of activated carbon to adsorb hydrogen.

Researchers from Northeastern University in Boston, MA, have recently announced that they have developed a carbon storage material that can store as high as 75% of hydrogen by weight [2]. This material, apparently some kind of carbon nanotubes or carbon whiskers is currently being researched in several laboratories. The best results achieved with carbon nanotubes to date confirmed by the National Renewable Energy Laboratory is hydrogen storage density corresponding to about 10% of the nanotube weight [3].

Hydrogen can be stored in glass microspheres of approximately 50 μm diameter. The microspheres can be filled with hydrogen by heating them to increase the glass permeability to hydrogen. At room temperature, pressure of approximately 25 MPa is achieved resulting in storage density of 14% mass fraction and 10 kg H_2/m^3 [4]. At 62 MPa a bed of glass microspheres can store 20 kg H_2/m^3. The release of hydrogen occurs by reheating the spheres to again increase the permeability.

Researchers at University of Hawaii are investigating hydrogen storage via polyhidride complexes. Complexes have been found which catalyze the reversible hydrogenation of unsaturated hydrocarbons. This catalytic reaction could be the basis for a low temperature hydrogen storage system with an available hydrogen density greater than 7% [5].

3.4 References

1. J.A. Schwartz and K.A.G. Amankwah, Hydrogen Storage Systems, in *The Future of Energy Gases*, D.G. Howell (ed.), U.S. Geological Survey Professional Paper 1570, pp. 725-736, U.S. Government Printing Office, Washington, 1993
2. *Hydrogen & Fuel Cell Letter*, Boston Team Claims Development of 5,000-Mile Range Onboard Hydrogen Storage Method, *HFCL*, Vol. XII, No. 2., pp. 1, 1997.
3. A.C. Dillon, K.M. Jones, and M.J. Heben, Carbon nanotube materials for hydrogen storage, Proc. 1996. U.S. DOE Hydrogen Program Review, Vol. II, pp. 747-763, NREL, Golden, CO, 1996
4. G. Rambach and C. Hendricks, Hydrogen Transport and Storage in Engineered Glass Microspheres, Proc. 1996. U.S. DOE Hydrogen Program Review, Vol. II, pp. pp. 765-772, NREL, Golden, CO, 1996
5. C. Jensen, Hydrogen Storage via Polyhydride Complexes, Proc. 1996. U.S. DOE Hydrogen Program Review, Vol. II, pp. pp. 787-794, NREL, Golden, CO, 1996

4. Fuel Cell Options – Trade-offs

Fuel cell can operate using either pure oxygen produced by the electrolyzer or oxygen from air. Oxygen operation has an advantage since it results in a higher fuel cell voltage and a simpler system. The disadvantage is that oxygen has to be stored, and storage and handling of oxygen requires special attention and it adds to the size of the system (oxygen storage size would be half of the hydrogen storage size if both gases are stored as compressed gases).

Instead of using pure oxygen the fuel cell may use air. In this case no oxygen storage and handling is required, but air has to be supplied to the fuel cell by means of a compressor or a blower. A fuel cell may operate at pressures ranging from atmospheric (101.3 kPA) to typically 308 kPa. Higher operating pressures have been reported but only when pure oxygen is used. Operating pressure or more precisely oxygen partial pressure has a significant impact on fuel cell performance which is best described by a polarization curve (cell voltage vs. current density). Operation at higher pressures results in voltage gain. Figure 4.1 shows the polarization curves of Energy Partners fuel cells operating on H2/O2 (at 308 kPa) and H2/air (at 308 and 136 kPa). It should be noted that only the portions of the curves are shown – those between 0.8 V and 0.6 V, which is actually a practical operating range.

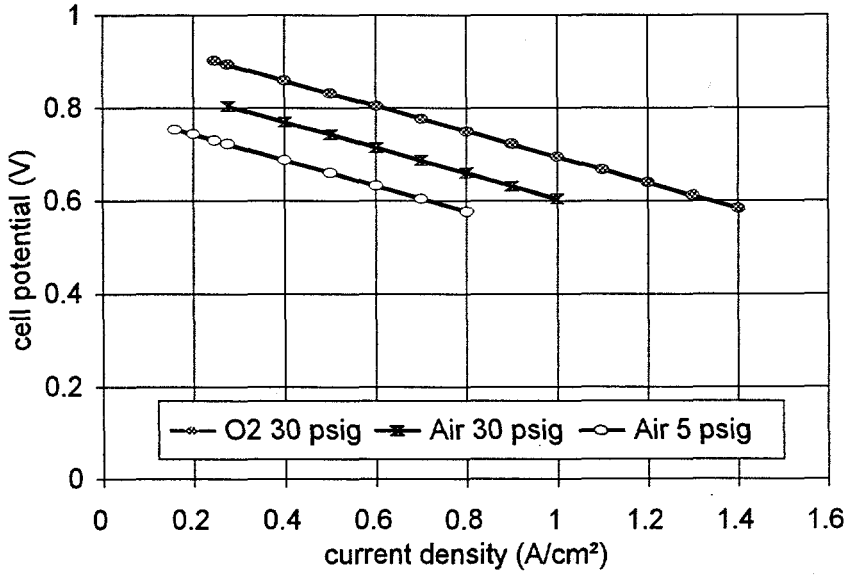

Figure 4.1 Linearized polarization curves of Energy Partners fuel cell stacks (292 cm^2 up to 110 cells/stack)

Air operation results in efficiency and power output penalty since a part of the fuel cell power output must be used to run the compressor. For that reason it may be beneficial to select a lower operating pressure since

Fuel cell polarization curve can for this analysis be approximated by a straight line (which is actually a very good approximation in the range between 0.8 and 0.6 V):

$$V_{cell} = V_o - k \cdot i \qquad \text{(Eq. 4.1)}$$

where:
V = cell voltage (V)
V_o = straight line intercept at i=0 (V)
k = slope (Vcm^2/A)
i = current density (A/cm^2)

Fuel cell stack power is a product of cell voltage, current density, active area and number of cells in the stack:

$$P_{fc} = V \cdot i \cdot A \cdot N_{cell} = (V_o - k \cdot i) \cdot i \cdot A \cdot N_{cell} \qquad \text{(Eq. 4.2)}$$

where:
P_{fc} = fuel cell power output (W)
A = cell active area (cm^2)
N_{cell} = number of cells in stack

Energy Partners' NG2000 fuel cell stack is based on a cell active area of 292 cm^2 and the stacks with up to 110 cells have been built to date. Figure 4.2 shows the power output of a NG2000 60-cell stack operating with pure oxygen and air. Since air has to be delivered to the fuel cell a part of the fuel cell power must be used to power the compressor or a blower. Therefore the net power is:

$$P_{net} = P_{fc} - P_{cmpr} \qquad \text{(Eq. 4.3)}$$

where:

$$P_{cmpr} = \dot{m}_{air} C_p T_{amb} \left[\left(\frac{p}{p_{amb}} \right)^{0.2857} - 1 \right] \frac{1}{\eta_{cmpr}} \qquad \text{(Eq. 4.4)}$$

where:
m_{air} = air mass flow rate (g/s)
C_p = air specific heat (J/g/°K)
T_{amb} = ambient temperature (°K)
p = operating pressure (bar)
p_{amb} = ambient pressure (bar)
η_{cmpr} = compressor efficiency

The air flow rate is proportional to current:

$$\dot{m}_{air} = \frac{I m_{O2}}{2nFg_{O2}} N_{cell} S \qquad \text{(Eq. 4.5)}$$

where:
I = current (A·i), Amps
m_{O2} = oxygen molecular weight (16 g/mol)
n = number of electrons involved in the reaction (2)
F = Faraday's constant = 96485 C/mol

g_{O2} = oxygen content in air by weight (0.232)
S = stoichiometric ratio

By combining equations 4.4. and 4.5 and numerical values for the constants:

$$P_{cmpr}=P_{cmpr} = 0.106 \cdot i \cdot A \cdot N_{cell} \cdot S \cdot \left[\left(\frac{p}{p_{amb}} \right)^{0.2857} - 1 \right] \frac{1}{\eta_{cmpr}} \qquad \text{(Eq. 4.6)}$$

The system efficiency is:

$$\eta_{sys} = \eta_{fc} \cdot \eta_{aux} = \frac{V_{cell}}{1.254} \frac{P_{fc} - P_{cmpr}}{P_{fc}} = \frac{V_{cell}}{1.254} \left(1 - \frac{P_{cmpr}}{P_{fc}} \right) \qquad \text{(Eq. 4.7)}$$

where:
η_{fc} = fuel cell efficiency
η_{aux} = efficiency related to auxiliary power requirements
V_{cell} = cell voltage
1.254 = voltage corresponding to hydrogen lower heating value

Figure 4.2 shows that the net power of a pressurized air fuel cell is actually lower than the net power of a low pressure fuel cell (some pressure is required at the fuel cell inlet to overcome the pressure drop through the stack).

Figure 4.3 shows the efficiency vs. power output for the three cases considered, namely H_2/O_2 at 308 kPa, H_2/air at 308 kPa and H_2/air at 136 kPa. In all three cases a 60-cell NG2000 fuel cell stack has been considered. A direct comparison is not possible since the three stacks have different power output. If 10 kW is a desired power output and number of cells in each stack is selected so that the stack generates 10 kW at 0.6 V/cell than the resulting efficiency vs. power curves and number of cells in each stack are shown in Figure 4.4. A H_2/O_2 fuel cell stack would require half of the cells of a H_2/air stack and would have higher system efficiency throughout the operating range. The efficiency of a fuel cell may be improved by adding more cells to the stack. Figure 4.5 compares the three stacks with the same power output (10 kW) and the same system efficiency at nominal power (44%). It should be noted that a pressurized air stack would require additional 51 cells to get the same system efficiency at 10 kW as a low pressure stack. A H_2/O_2 stack would require only additional 3 cells to improve the system efficiency from 44% to 50%, a low pressure H_2/air stack would need 36 additional cells (121 total) and a pressurized stack would require more than twice as many cells to make the same efficiency gain (Figure 4.6).

It should be noted that the efficiency and power output of a pressurized air stack may be improved by incorporating an expander in the system that could recover some power from the pressurized and depleted air coming out of the fuel cell stack. This option is being considered for automotive fuel cell systems.

From this simplified analysis (other parasitic losses have been neglected here) it appears that H_2/O_2 fuel cell would be smaller and more efficient than comparable H_2/air fuel cell. However, the ultimate criteria for selection of the type of fuel cell should be the cost of the final product,

i.e., the cost of kWh of electricity delivered. Therefore, a detailed cost analysis is required that would take into account the capital cost of the fuel cell and blower on one side and oxygen storage and oxygen recirculation pump on the other side, as well as the efficiencies of the systems to be compared.

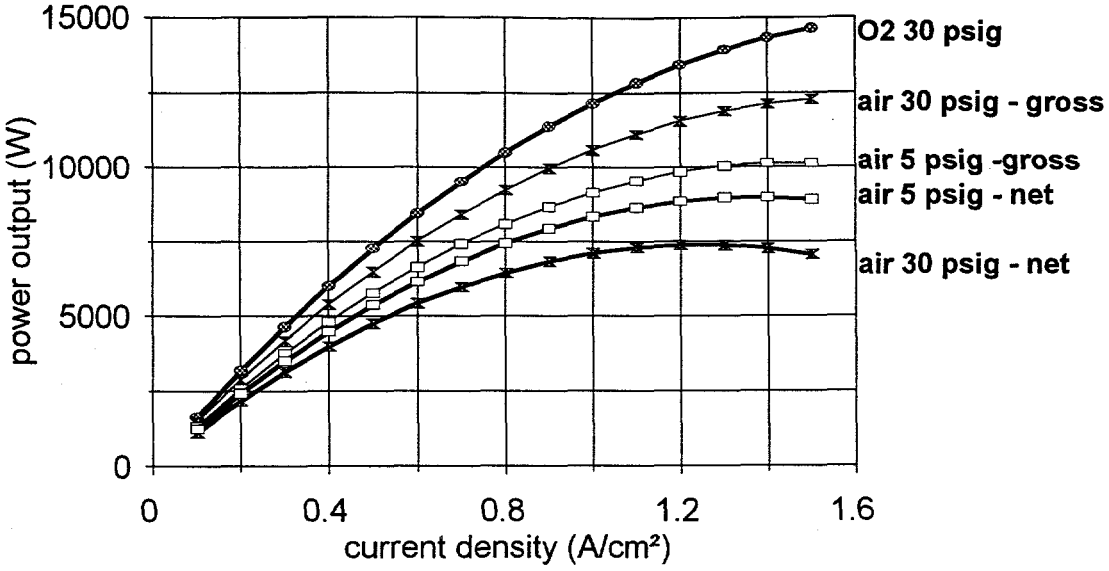

Figure 4.2 Power output of 60-cell stacks (292 cm^2) with performance corresponding to Figure 4.1

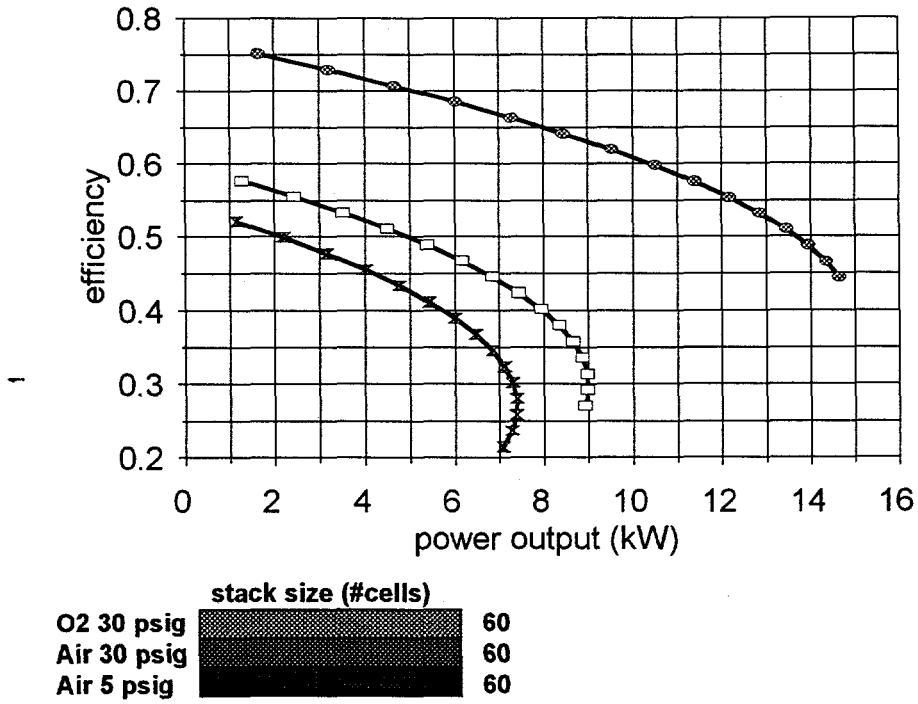

Figure 4.3 System efficiency vs. power output for stacks from Figures 4.1 and 4.2

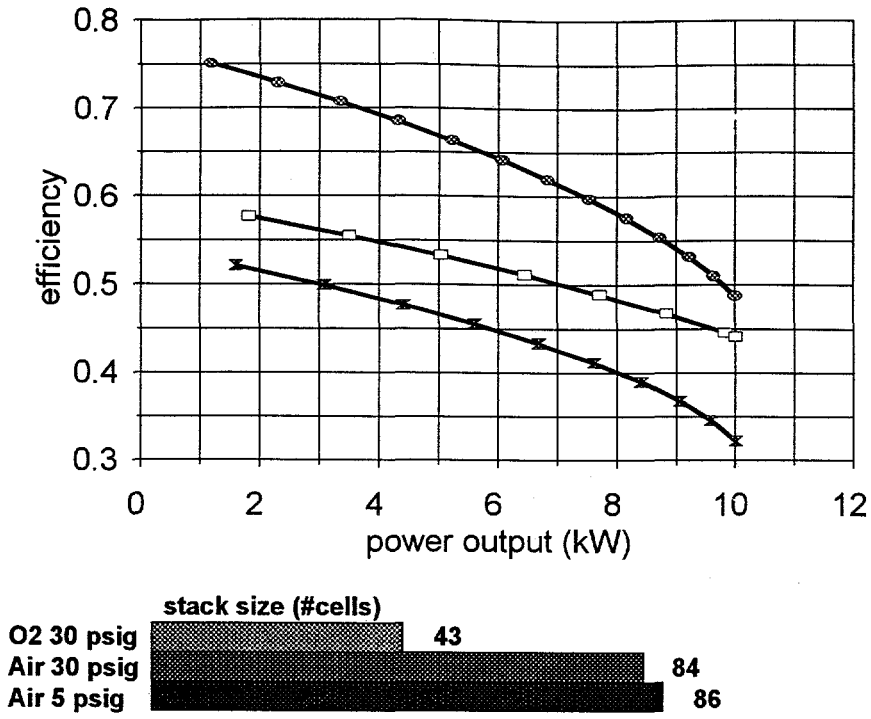

Figure 4.4 Efficiency vs. power output for stacks from Figures 4.1 and 4.2 and resulting number of cells needed to generate 10 kW at 0.6 V/cell

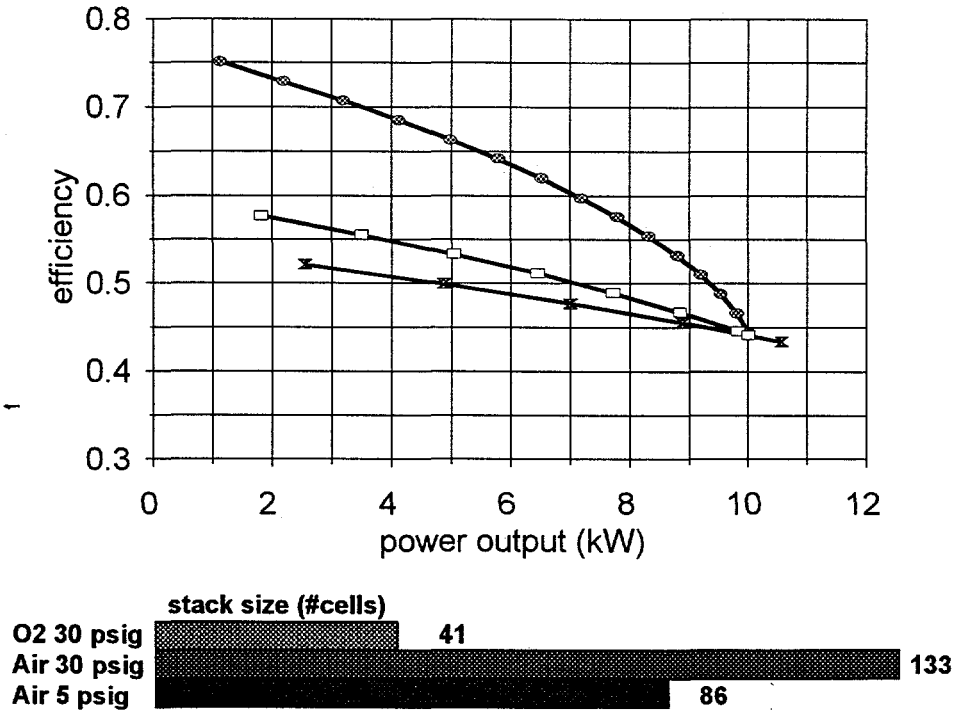

Figure 4.5 Efficiency vs. power output for stacks from Figures 4.1 and 4.2 and resulting number of cells needed to generate 10 kW at 50% system efficiency

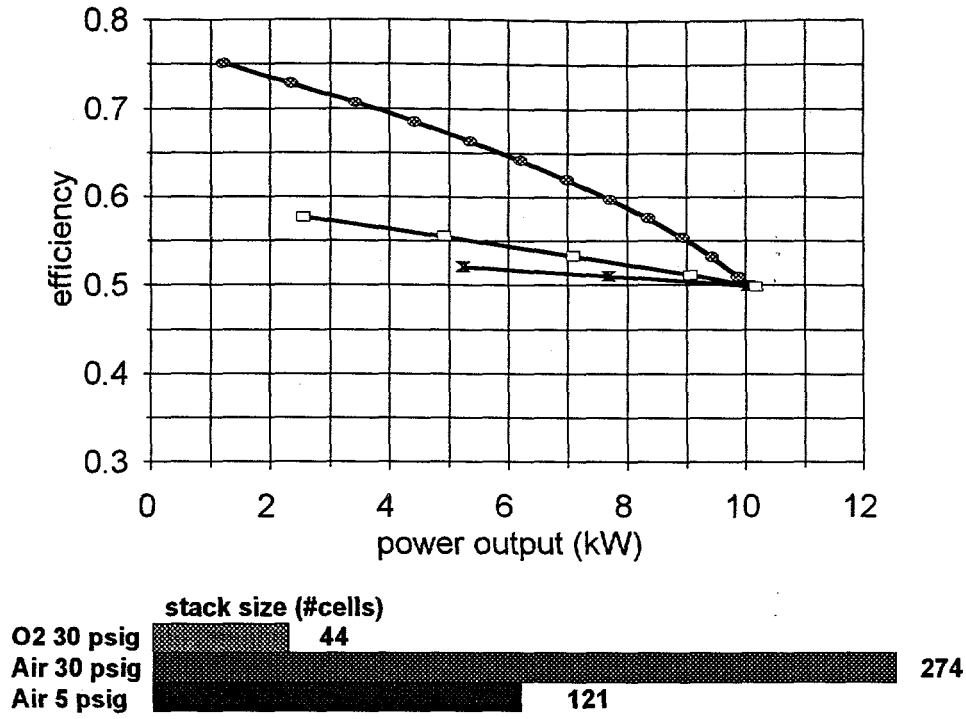

Figure 4.4 Efficiency vs. power output for stacks from Figures 4.1 and 4.2 and resulting number of cells needed to generate 10 kW at 50% system efficiency

5. Application Considerations and Techno-Economic Analysis

The integrated renewable hydrogen utility system is supposed to be used in conjunction with a renewable source such as photovoltaic array or wind generator. In general, with a few exemptions the renewable power sources are only intermittently available. Their availability is dictated by the forces of nature. Therefore they cannot be used directly to cover the load, which in general also varies with time. Figure 5.1 shows an example of a variable load. A renewable power source can be used directly to cover a part of the load (Figure 5.1a). The rest must be covered from other, more controllable, sources. A relatively large renewable power source (Figure 5.1.b) may be used to cover some of the load, but there is excess power available which would have to be stored in some way and eventually used to cover more of the load. However, power from the renewable source is not enough to cover the entire load, and the rest must be covered from other sources. The third possibility is that the renewable power source is sized so that it can cover the entire load either directly or indirectly (Figure 5.1c). As such it is used as the only power source.

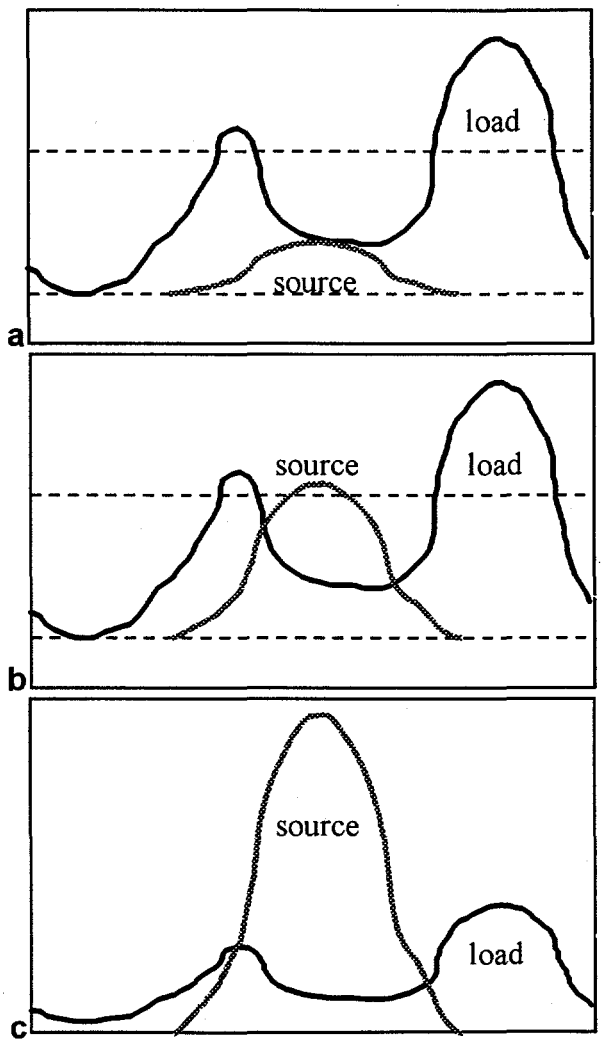

Figure 5.1 Mismatch between renewable power source and load

An integrated renewable hydrogen utility system has no application in Case a, since there is no need for energy storage. It could be used in Case "b" but only in conjunction with other power sources. On a macro utility scale it would have to be used with a large renewable power source and would require fuel cells and electrolyzer on a MW level. It could also be used on a micro-level, covering smaller loads (on the order of magnitude of 1 to 100 kW) but in that case the cost of power generated directly would have to compete with the cost of off-peak grid electricity, and the cost of indirectly (after being stored) generated power would have to compete with the cost of peak electricity. The integrated renewable hydrogen utility system makes best sense in Case "c" when the renewable source is practically the only available source. This is the case of remote locations, isolated communities, islands, etc., with power levels in the order of magnitude of 1 to 100 kW.

The following analysis of an idealized case has been perform in order to get an idea on relative nominal power inputs and outputs, system efficiencies and capacity factors which will then be used in the economic analysis.

For the electrolyzer/fuel cell system these parameters are related to each other. The relative nominal power outputs and capacity factors are dictated by the power profiles of both the available power source and load. This will vary from location to location and from application to application. In general, renewable sources, such as solar and wind, are available intermittently with daily and seasonal variations. The integrated renewable hydrogen utility system is supposed to use power from a renewable source and deliver it to the load either directly or indirectly.

In general there are three modes of operation of the system, as shown in Figure 5.2:

- during periods when renewable power is not available – power to the load is provided by the fuel cell
- during periods when renewable power is available but not sufficient to cover the load – power to the load is provided from both source and fuel cell
- during periods when renewable power exceeds load – power to the load is provided directly from the source and excess (if any) is used by the electrolyzer to generate hydrogen

The source power profile is assumed to have a sinusoidal form typical for solar power availability (Figure 5.2). Energy from the renewable power source, E_S, must be sufficient to cover the load plus all the losses in energy conversions. Energy from the renewable source is proportional to its maximum power, $P_{S\text{-}MAX}$, and it is a function of load profile:

$$E_S = \int_0^{24} P_S(t)dt = P_{S-MAX} \int_0^{24} \frac{P_S}{P_{S-MAX}}(t)dt \qquad \text{(Eq. 5.1)}$$

Since the renewable source operates with a low capacity factor (typically 0.20-0.25) its power must exceed the load power. In this analysis the load is assumed to be constant 10 kW.

$$P_L = 10 \text{ kW} \qquad \text{(Eq. 5.2)}$$

Energy consumed by the load is:

$$E_L = \int_0^{24} P_L dt = 24P_L \qquad \text{(Eq. 5.3)}$$

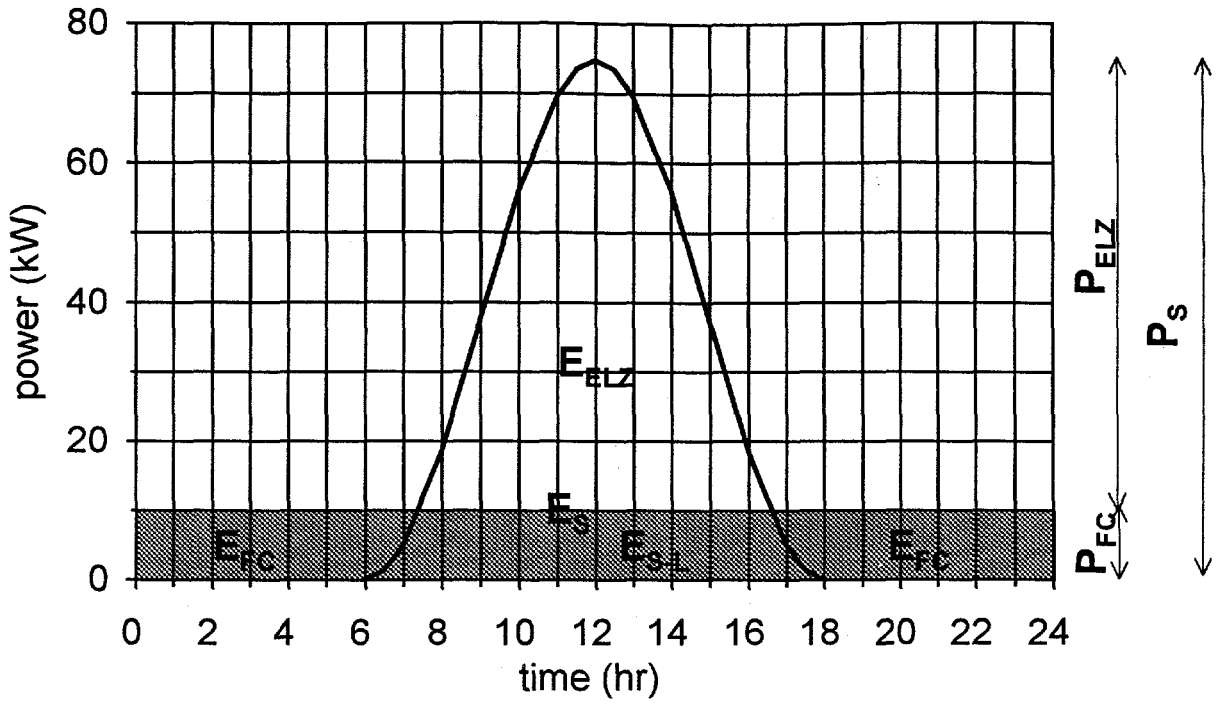

Figure 5.2 Idealized source and load profiles

The fuel cell must be capable of satisfying the load so its power, P_{FC}, must match the load power:

$$P_{FC} = P_L \quad \text{(Eq. 5.4)}$$

The fuel cell provides only part of the energy consumed by the load (E_{FC}); the remaining part is supplied directly from the renewable source (E_{S-L}):

$$E_L = E_{FC} + E_{S-L} \quad \text{(Eq. 5.5)}$$

Energy supplied directly from the source to the load can be calculated from source and load power profiles:

$$E_{S-L} = f\left(P_L, P_{S-MAX}, \frac{P_S}{P_{S-MAX}}(t)\right) \quad \text{(Eq. 5.6)}$$

The excess power from the source not being used by the load is used in the electrolyzer to generate hydrogen:

$$E_S = E_{ELZ} + E_{S-L} \quad \text{(Eq. 5.7)}$$

Electrolyzer's power is therefore:

$$P_{ELZ} = P_{S-MAX} - P_L \quad \text{(Eq. 5.8)}$$

Energy used in the electrolyzer is converted to hydrogen and stored:

$$E_{H2} = E_{ELZ}\eta_{ELZ} \quad \text{(Eq. 5.9)}$$

Hydrogen is then used in the fuel cell to generate electricity:

$$E_{FC} = E_{H2}\eta_{FC} \qquad \text{(Eq. 5.10)}$$

The above equations represent a self-consistent set that can be solved analytically or numerically depending on the form of source and load power profiles. For this idealized case they have been solved as a function of fuel cell and electrolyzer efficiencies.

For sizing purposes it is interesting to know the ratio between the electrolyzer and fuel cell power. Figure 5.3 shows this ratio as a function of fuel cell and electrolyzer efficiencies. In general, the higher fuel cell and electrolyzer efficiencies are less energy is needed from the source and consequently the lower electrolyzer power is required. For the range of analyzed fuel cell and electrolyzer efficiencies (0.45-0.55 and 0.75-0.85 respectively) the electrolyzer's nominal power varies from 7.5 to 5.6 times the fuel cell nominal power. This is actually the maximum ratio that can be expected because of the assumed constant load. In the cases with a variable load this electrolyzer/fuel cell power ratio may be considerable smaller, but the fuel cell capacity factor would be considerably lower.

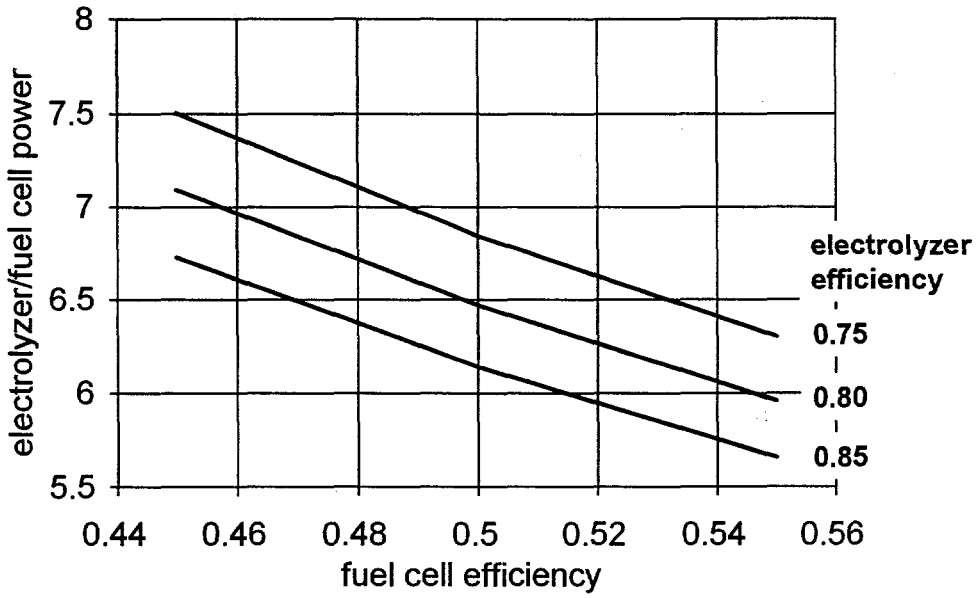

Figure 5.3 Electrolyzer/fuel cell power ratio

The fuel cell capacity factor is defined as ratio of actually produced electricity in a given time period (in this case 24 hours) and electricity that could have been produced if the fuel was operated full power during the same time period:

$$CF_{FC} = \frac{E_{FC}}{24 \cdot P_{FC}} \qquad \text{(Eq. 5.11)}$$

Similarly, the electrolyzer capacity factor is defined as ratio of actually consumed electricity by the electrolyzer in a given time period and electricity that could have been consumed if the electrolyzer was operated full power during the same time period:

$$CF_{ELZ} = \frac{E_{ELZ}}{24 \cdot P_{ELZ}} \qquad \text{(Eq. 5.12)}$$

Figure 5.4 shows that both the fuel cell and the electrolyzer capacity factors are fairly independent of the fuel cell and electrolyzer efficiencies, and for this case the fuel cell capacity factor was about 58% and the electrolyzer capacity factor was about 22.5%. Because of the assumed constant load this is actually the highest fuel cell capacity factor possible with the assumed source power profile. The electrolyzer capacity factor is very low, and it can be increased in the cases where more load can be satisfied directly from the source.

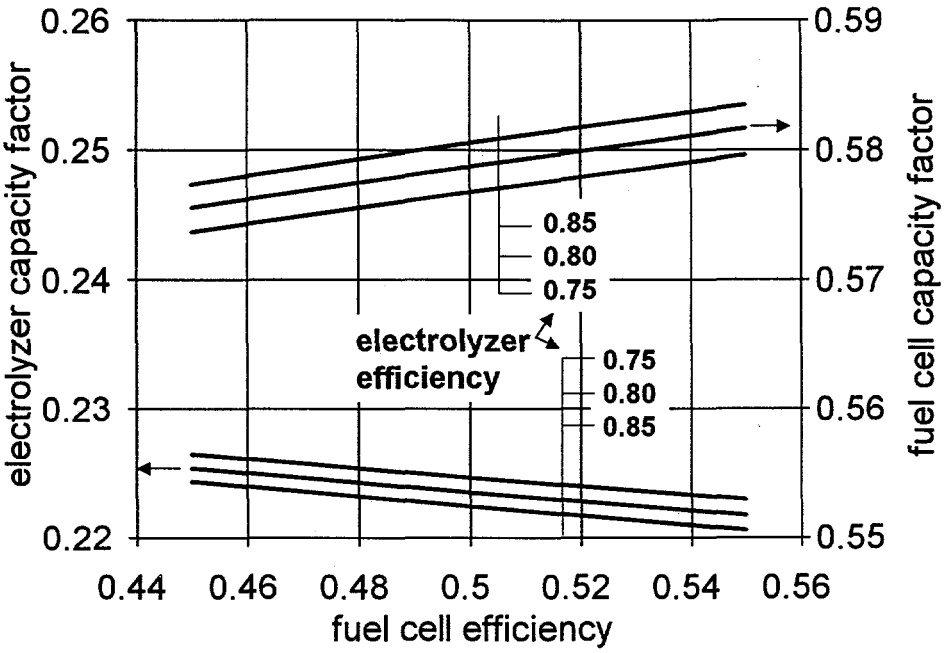

Figure 5.4 Electrolyzer and fuel cell resulting capacity factors

The total system efficiency may be defined as a ratio between produced and consumed energy:

$$\eta_{SYS} = \frac{\text{energy out}}{\text{energy in}} = \frac{E_L}{E_S} \qquad \text{(Eq. 5.13)}$$

The resulting system efficiency is shown in Figure 5.5. As expected it is a strong function of fuel cell and electrolyzer efficiencies. It is higher than the round-trip conversion efficiency ($\eta_{fc}\eta_{elz}$) because a part of the delivered energy comes directly from the source (power conditioning losses, if any, have been neglected in this analysis).

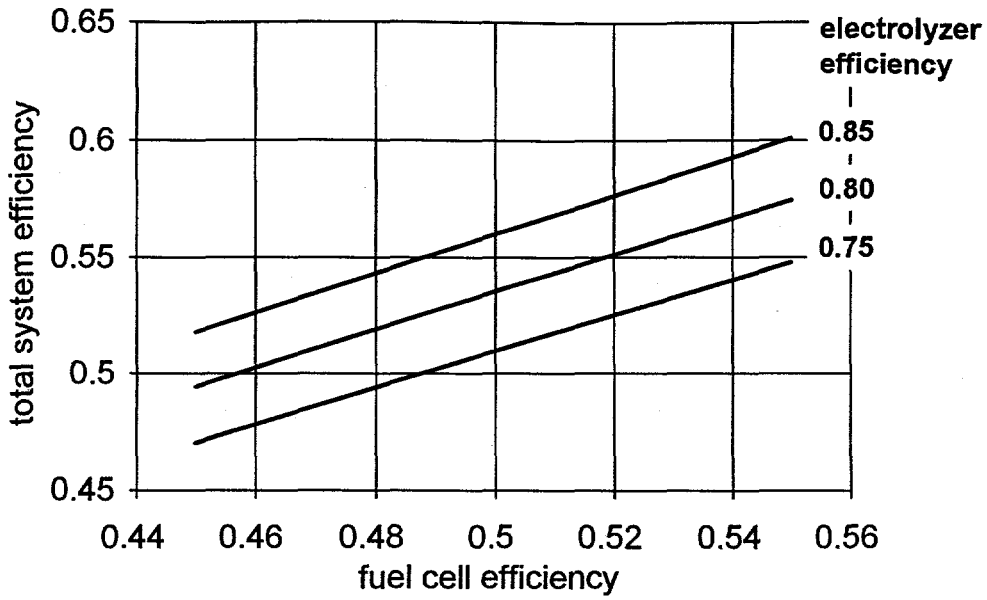

Figure 5.5 Resulting total system efficiency

6. Optimization of Fuel Cell and Electrolyzer Size and Efficiency

6.1. Introduction

Both the fuel cell and the electrolyzer have the feature that the efficiency may be increased by adding more cells. In fuel cell, this results in increased cell voltage for a given power output, and therefore in increased efficiency. In electrolyzer, this results in lower cell voltage which again results in increased efficiency. Increased efficiency of both fuel cell and electrolyzer means lower operating costs. However, additional cells mean higher capital cost. Therefore, there must be an optimum fuel cell and electrolyzer voltage that would result in the lowest total cost, i.e., cost of delivered electricity in $/kWh.

6.2. Methodology

Cost of delivered electricity (in $/kWh) is:

$$C_{el}^{out} = \frac{ACC + AOC}{AED} \qquad \text{(Eq. 6.1)}$$

where:
ACC = annualized capital cost ($/yr)
AOC = annual operating cost ($/yr)
AED = annual amount of electricity delivered (kWh/yr)

$$AAC = FCR \cdot SCC \qquad \text{(Eq. 6.2)}$$

where:
FCR = fixed charge rate (yr^{-1})
SCC = system capital cost ($)

$$SCC = CC_{fc} + CC_{elz} \qquad \text{(Eq. 6.3)}$$

where:
CC_{elz} = electrolyzer capital cost
CC_{fc} = fuel cell capital cost

$$CC_{fc} = (C_{stack} + C_{cell} \cdot N_{cell})_{fc} \qquad \text{(Eq. 6.4)}$$

where:
C_{stack} = fixed cost per fuel cell stack
C_{cell} = cost per cell
N_{cell} = number of cells in the stack

$$N_{cell}^{fc} = \frac{P_{fc} \cdot 1000}{V_{cell}^{fc} \cdot i_{fc} \cdot A_{fc}} \qquad \text{(Eq. 6.5)}$$

where:
P_{fc} = fuel cell nominal power (kW)
i_{fc} = fuel cell current density (A/cm^2)
A_{fc} = fuel cell active area (cm^2)
V_{cell}^{fc} = fuel cell cell voltage (V)

$$V_{cell}^{fc} = V_o^{fc} - k_{fc} \cdot i_{fc} \qquad \text{(Eq. 6.6)}$$

where:
V_o = polarization curve intercept voltage (V)
k = polarization curve slope (V/A)
i_{fc} = fuel cell current density (A/cm^2)

CC_{elz} = electrolyzer capital cost

$$CC_{elz} = (C_{stack} + C_{cell} \cdot N_{cell})_{elz} \qquad \text{(Eq. 6.7)}$$

where:
C_{stack} = fixed cost per electrolyzer stack
C_{cell} = cost per cell
N_{cell} = number of cells in the stack

$$N_{cell}^{elz} = \frac{P_{elz} \cdot 1000}{V_{cell}^{elz} \cdot i_{elz} \cdot A_{elz}} \qquad \text{(Eq. 6.8)}$$

where:
P_{elz} = electrolyzer nominal power (kW)
i_{elz} = electrolyzer current density (A/cm^2)
A_{elz} = electrolyzer cell active area (cm^2)
V_{cell}^{elz} = electrolyzer cell voltage (V)

$$V_{cell}^{elz} = V_o^{elz} + k_{elz} \cdot i_{elz} \qquad \text{(Eq. 6.9)}$$

where:
V_o = polarization curve intercept voltage (V)
k_{elz} = polarization curve slope (V/A)
i_{elz} = electrolyzer current density (A/cm^2)

P_{elz} = electrolyzer nominal power (kW)

$$P_{elz} = \frac{P_{fc} CF_{fc}}{CF_{elz}} \frac{V_{cell}^{elz}}{V_{cell}^{fc}} \qquad \text{(Eq. 6.10)}$$

where:
P_{fc} = fuel cell nominal power (kW)
CF_{fc} = fuel cell capacity factor
CF_{elz} = electrolyzer capacity factor
V_{cell}^{fc} = fuel cell cell voltage (V)
V_{cell}^{elz} = electrolyzer cell voltage (V)

AOC = annual operating cost ($/yr)

$$AOC = AEC \cdot C_{el}^{in} \qquad \text{(Eq. 6.11)}$$

where:

C_{el}^{in} = cost of electricity from renewable source ($/kWh)
AEC = annual electricity consumed (kWh/yr)

$$AEC = \frac{AED}{\eta_{fc}\eta_{elz}} = AED\frac{V_{cell}^{elz}}{V_{cell}^{fc}} \qquad \text{(Eq. 6.12)}$$

where:
AED = annual amount of electricity delivered (kWh/yr)
η_{fc} = fuel cell efficiency
η_{elz} = electrolyzer efficiency

AED = annual amount of electricity delivered (kWh/yr)

$$AED = P_{fc} \cdot CF_{fc} \cdot 8760 \qquad \text{(Eq. 6.13)}$$

where:
P_{fc} = fuel cell nominal power (kW)
CF_{fc} = fuel cell capacity factor
8,760 = hours/yr

6.3. Inputs, assumptions and variables

The optimization analysis was performed with the following set of assumptions:

- fuel cell polarization curves: linearized from EP data (see Figure 4.1)
- electrolyzer polarization curve: linearized from Treadwell data (see Figure 3.4)
- fixed charge rate (capital recovery factor): 0.15/yr (corresponding to lifetime of 10 years and discount rate of 7.5%)
- fuel cell capacity factor: 0.58
- electrolyzer capacity factor: 0.22
- fuel cell nominal power output: 10 kW
- only fuel cell and electrolyzer costs were taken into account

The following parameters were used as variables:

- fuel cell present cost (based on 300 cm^2 active area):
  - fixed cost per stack: $8,000
  - cost per cell: $800
  - total costs corresponding to about $5,000/kW
- fuel cell future cost (based on 300 cm^2 active area):
  - fixed cost per stack: $1,700
  - cost per cell: $170
  - total costs corresponding to about $1,000/kW
- fuel cell mass production cost (based on 300 cm^2 active area):
  - fixed cost per stack: $200
  - cost per cell: $10
  - total costs corresponding to less than $100/kW
- electrolyzer present cost (based on 200 cm^2 active area):

    - fixed cost per stack: $8,000
    - cost per cell: $800
- electrolyzer future cost (based on 200 cm^2 active area):
    - fixed cost per stack: $2,000
    - cost per cell: $200
- fuel cell nominal cell voltage: 0.6V – 0.8 V
- electrolyzer nominal cell voltage: 1.8V – 2.2V
- cost of electricity from renewable source: $0.02-$0.20/kWh

6.4. Results

The results of this analysis are shown in Figures 6.1-6.9. At current fuel cell and electrolyzer costs the cost of delivered electricity is prohibitively expensive:

- about $1/kWh if the cost of input electricity is $0.20/kWh (Figure 6.1)
- $0.5/kWh if the cost of input electricity is $0.05/kWh (Figure 6.2), and
- $0.4/kWh if the cost of input electricity is $0.02/kWh (Figure 6.3).

The results indicate that the lowest cost is achieved when the fuel cell is sized at about 0.7 V/cell, except in the case with a highest cost of input electricity when the optimal fuel cell voltage is >0.8V/cell. The electrolyzer optimum voltage is found to be 2.2 Volts/cell, which results in relatively low electrolyzer efficiency. This is due to the electrolyzer's low capacity factor which makes the electrolyzer capital cost more dominant than the operating cost. In other words, the size of the electrolyzer has greater effect on the total cost than its efficiency.

Figure 6.4 summarizes the results for this expensive case. Electrolyzer and fuel cell costs are about the same.

The resulting electricity cost is somewhat lower for the projected/future fuel cell and electrolyzer capital costs:

- about $0.60/kWh if the cost of input electricity is $0.20/kWh (Figure 6.5)
- $0.21/kWh if the cost of input electricity is $0.05/kWh (Figure 6.6), and
- $0.13/kWh if the cost of input electricity is $0.02/kWh (Figure 6.7).

Optimum fuel cell and electrolyzer voltages are about the same as in the high cost scenario 0.7-0.8V/cell for the fuel cell and 2.0-2.2V/cell for the electrolyzer. The total cost is less sensitive to the selected nominal operating voltage. As shown in Figure 6.8, the cost of input electricity, even at $0.02/kWh is the highest contributing factor to the cost of delivered electricity.

Figure 6.9 shows almost linear relationship between the cost of input electricity and the cost of delivered electricity for the two cases, namely present and future fuel cell and electrolyzer costs. An additional scenario is added in which the fuel cell cost is assumed to be as low as required for automotive applications (>$100/kW). However, this scenario does not reduce the cost of delivered electricity significantly. This is due to the electrolyzer's high costs and low capacity factor. It should be noted that the extremely low fuel cell scenario is likely if (or when) the fuel cells are mass produced for automotive applications. Unfortunately, there is no similar scenario for the electrolyzers.

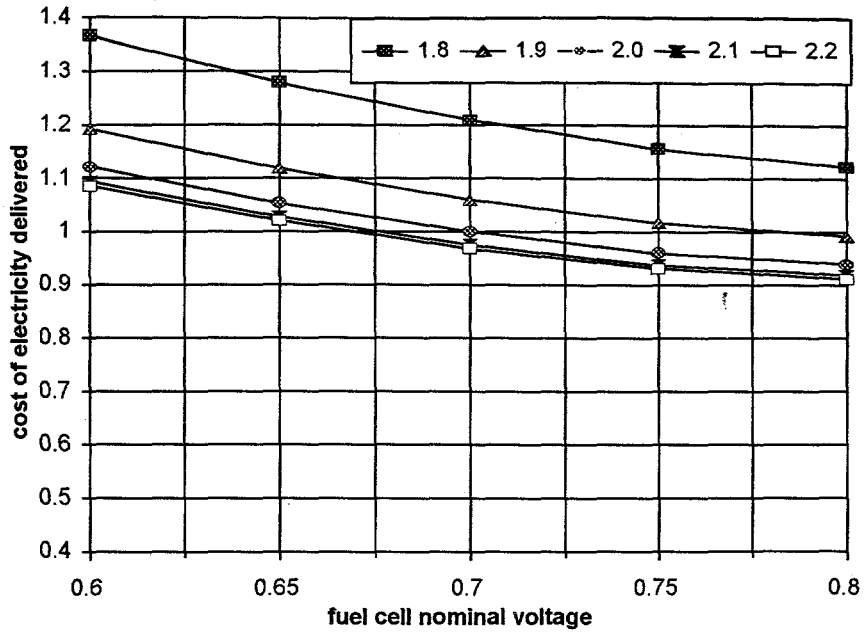

Figure 6.1 Cost of delivered electricity as a function of fuel cell nominal voltage (x-axis) and electrolyzer nominal voltage (legend) for current costs scenario and cost of electricity from renewable power source $0.20/kWh

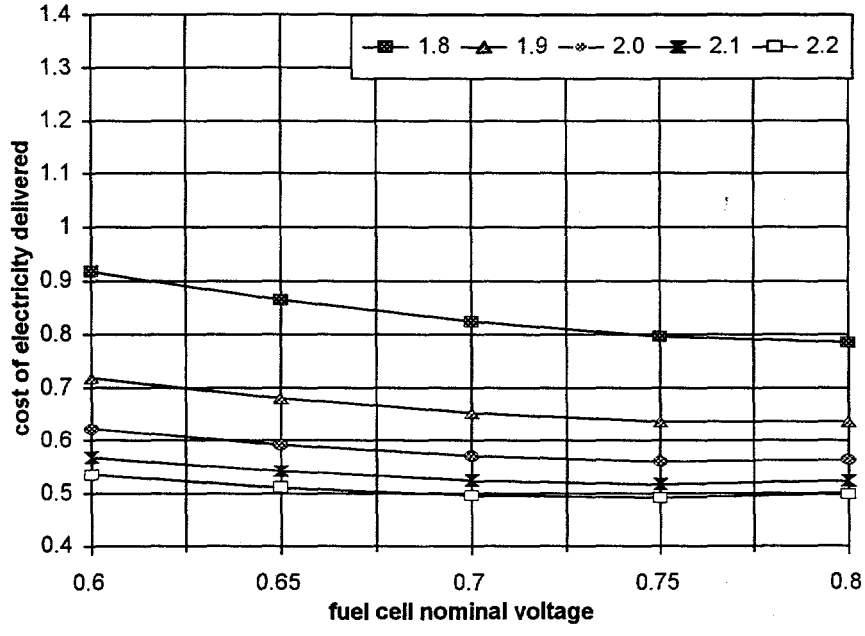

Figure 6.2 Cost of delivered electricity as a function of fuel cell nominal voltage (x-axis) and electrolyzer nominal voltage (legend) for current costs scenario and cost of electricity from renewable power source $0.05/kWh

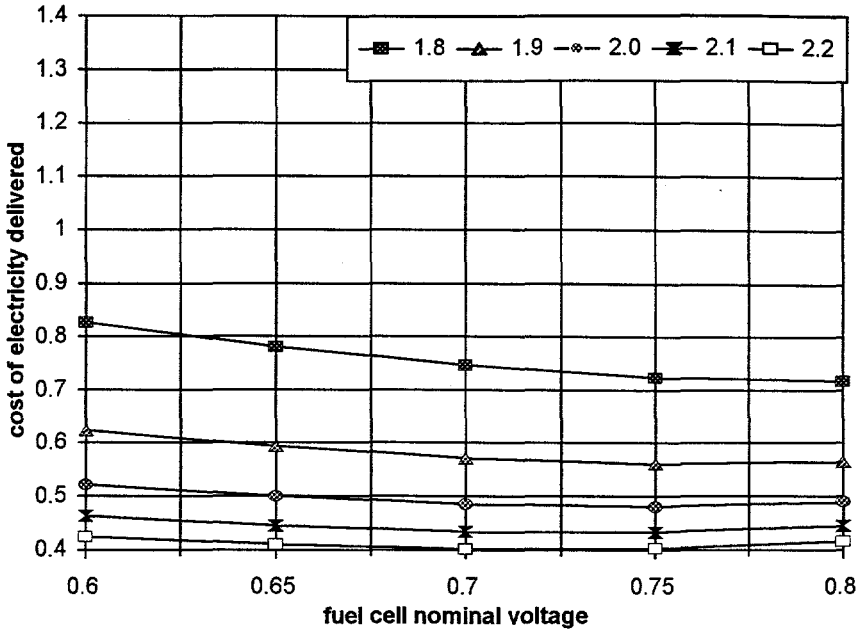

Figure 6.3 Cost of delivered electricity as a function of fuel cell nominal voltage (x-axis) and electrolyzer nominal voltage (legend) for current costs scenario and cost of electricity from renewable power source $0.02/kWh

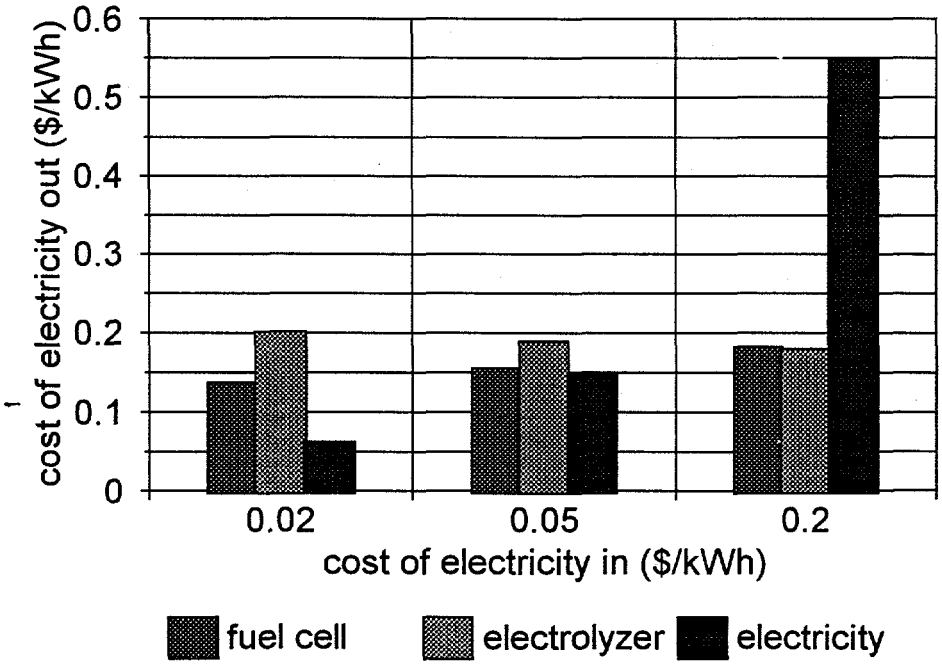

Figure 6.4 Breakdown of the cost of delivered electricity for current costs scenario

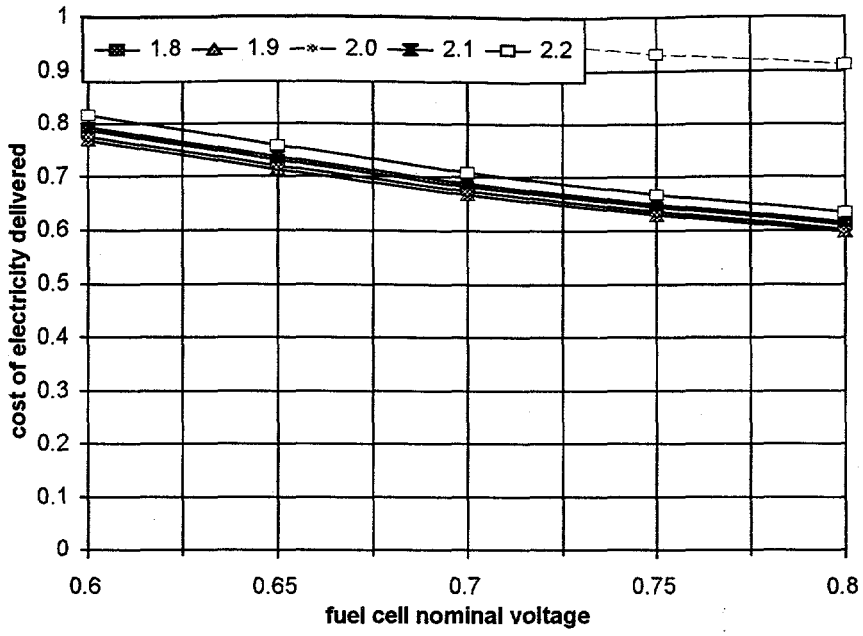

Figure 6.5 Cost of delivered electricity as a function of fuel cell nominal voltage (x-axis) and electrolyzer nominal voltage (legend) for future costs scenario and cost of electricity from renewable power source $0.20/kWh

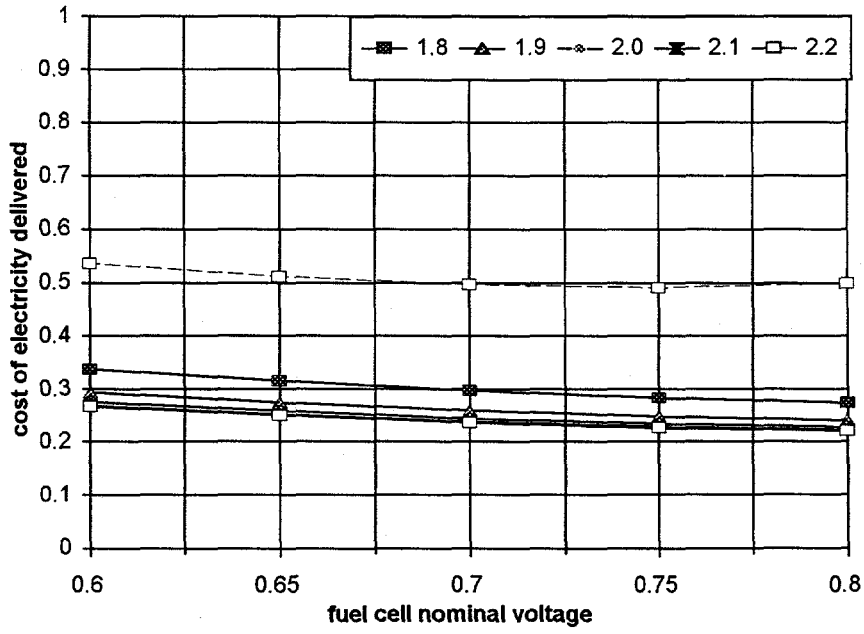

Figure 6.6 Cost of delivered electricity as a function of fuel cell nominal voltage (x-axis) and electrolyzer nominal voltage (legend) for future costs scenario and cost of electricity from renewable power source $0.05/kWh

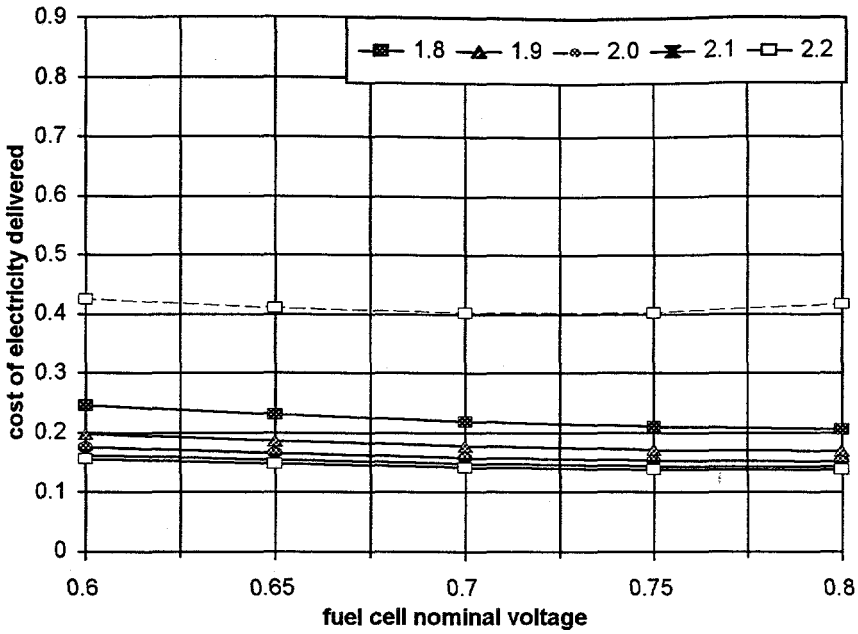

Figure 6.7 Cost of delivered electricity as a function of fuel cell nominal voltage (x-axis) and electrolyzer nominal voltage (legend) for future costs scenario and cost of electricity from renewable power source $0.02/kWh

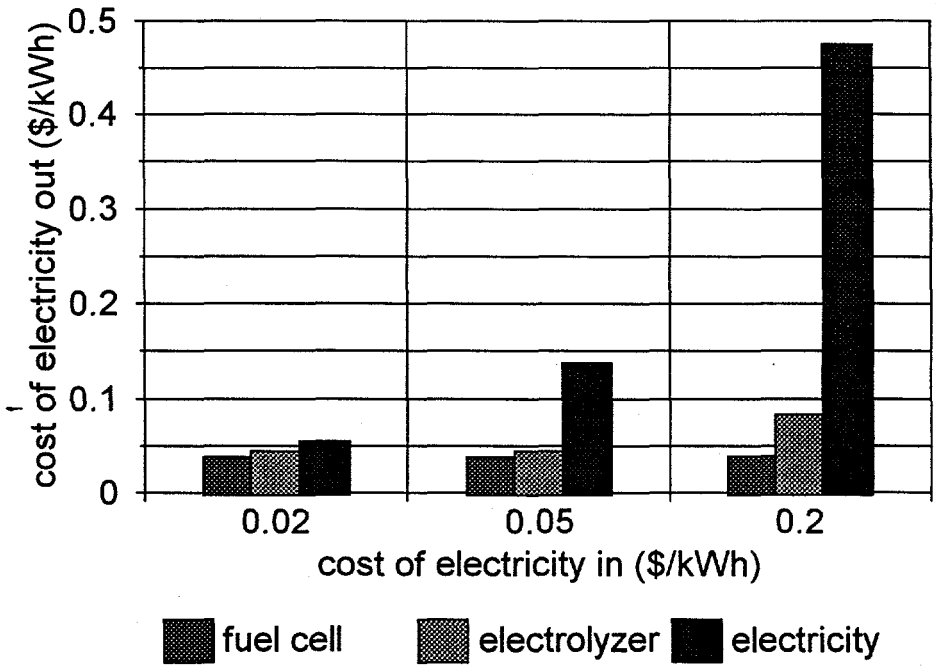

Figure 6.8 Breakdown of the cost of delivered electricity for future costs scenario

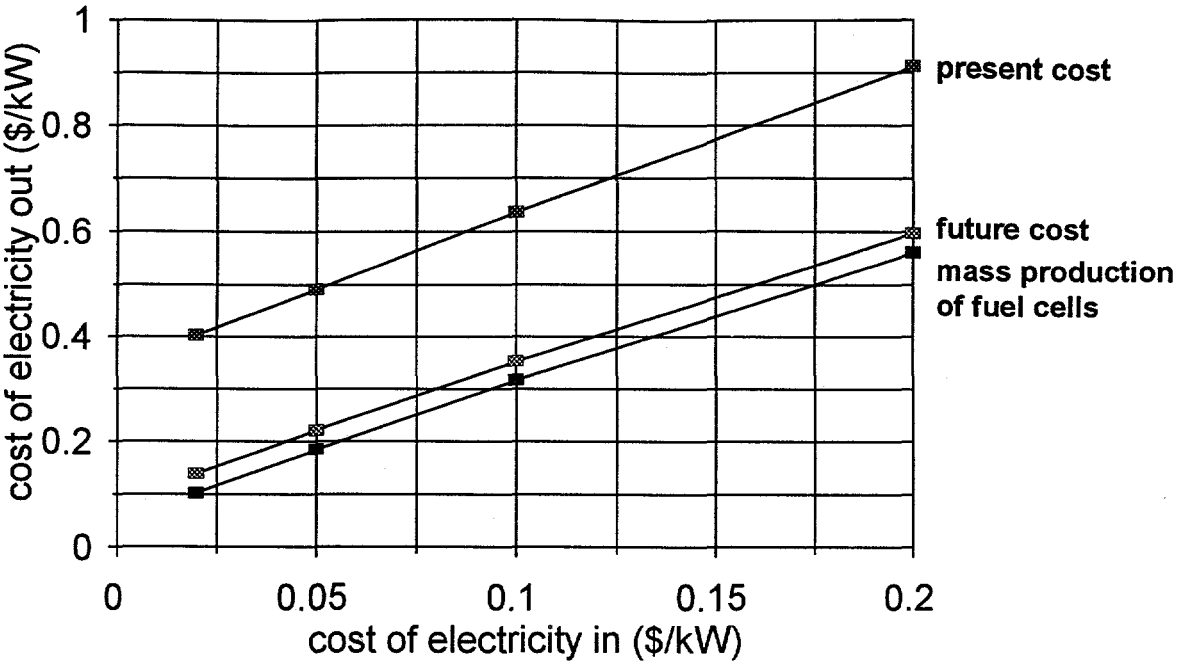

Figure 6.9 Cost of delivered electricity as a function of the cost of electricity input from the renewable power source for different scenarios

7. System Performance Simulation

This section was prepared by the Florida Solar Energy Center.

7.1 Introduction

The main goal of the system integration and computer simulation task is to develop an efficient tool to assist in the design and evaluation of the integrated renewable hydrogen utility systems (IRHUS). We have conducted an extensive literature search on different IRHUS demonstration projects (for example, references [1-5]). Selection of the demonstration projects was limited to IRHUS that comprises at least four major components: a PV-array, an electrolyzer, a fuel cell and a hydrogen storage unit. Our library of IRHUSs currently includes more than 50 entries. The following countries have on-going IRHUS programs: USA, Germany, Italy, Finland, Switzerland, Spain and South Korea. The power output of existing IRHUS demonstration projects varies from 1 to 350 kW.

We have also conducted a literature search for the existing computer simulation software packages (CSP). These software packages are designed to provide system developers with the component models and integrating platform through which these models can be linked into the conceptual design of the integrated energy system.

7.2 Computer simulation programs for IRHUS

Many of these demonstration projects have involved the utilization or creation of computer software to aid in the design and simulation of the IRHUS systems. Table 7.1 summarizes the results of a literature search for such simulation tools. Although there are certainly a large number of software packages that could be applied to the design of such a system, the literature search was limited to software whose applicability has already been evaluated.

Table 7.1: Existing Computer Simulation Programs for IRHUS

No	Title of CSP	Institution	Comment
1.	AspenPlus	NREL (USA)	Hydrogen included
2.	HOMER	NREL (USA)	Hydrogen not included
3.	Hybrid2	NREL (USA)	Hydrogen not included
4.	HHSSAPPS	Sandia NL (USA)	Hydrogen included
5.	PVSYST	Univ. Geneva (Switz.)	Hydrogen not included
6.	JULSIM	RC Julich (Germany)	Hydrogen not included
7.	TRNSYS	SEL/UW (USA)	Hydrogen included
8.	H2PHOTO	Univ.Helsinki (Finland)	Hydrogen included
9.	WATSUN	WSL (USA)	Hydrogen not included
10.	INTERSIM	RC Julich (Germany)	Hydrogen included

7.3 Description of the simulation software

After researching the performance of each type of simulation software, and their applicability towards modeling the proposed IRHUS, we chose TRNSYS, created by the Solar Energy Laboratory at the University of Wisconsin-Madison, to be the main platform for the system integration and simulation task. Although there is no software currently available that was designed with the intent of modeling such a system; there are examples in the literature where researchers have modified existing platforms to incorporate components of the IRHUS. Modification and use of the TRNSYS software is well documented and has produced reliable results.

TRNSYS is transient simulation software with source code written in FORTRAN. The transient nature of the program, where time is an inherent variable, is beneficial to this project for it allows the user to track system performance over the course of an entire year, with changing weather conditions and energy load profiles. The software is component driven, and many of the standard components available are needed for IRHUS simulation.

No models for the core components of the IRHUS (fuel cell, electrolyzer, and hydrogen storage) are currently included with the standard version of the TRNSYS software. However, the Solar Energy Laboratory has collected many applicable component models, written by various users, and is currently trying to incorporate them into the standard version of the program. The component models are now only used as a demonstration of the capabilities of TRNSYS, for much work needs to be done on their documentation before they can be integrated with the main source code. A schematic of the system used in the demonstration, called PVHYDRO, is shown in Figure 7.1.

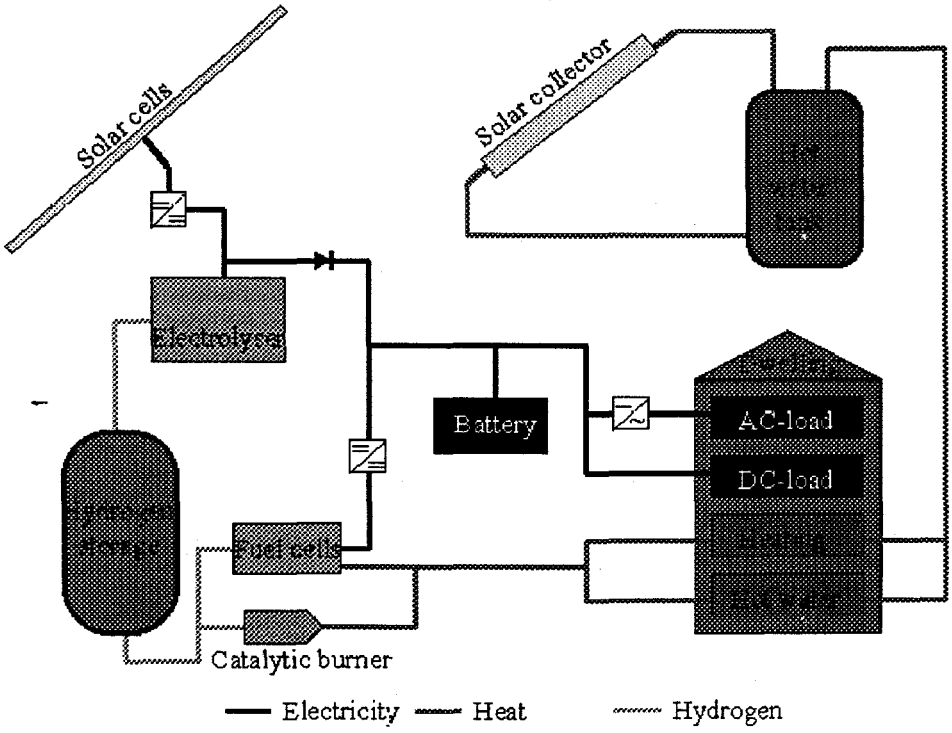

Figure 7.1: Schematic of PVHYDRO Demonstration

7.3.1 Description of PVHYDRO Demonstration

The system that the Solar Energy Laboratory has used as a basis for development of the PVHYDRO demonstration simulation is very similar in function to the proposed IRHUS. The main difference between the proposed IRHUS and PVHYDRO is the system application; namely end use of renewable energy generated by the system. PVHYDRO has been developed specifically to supply all the energy needs of a single-family dwelling. This dwelling is assumed to be equipped with both AC and DC appliances, therefore all DC electricity generated by the renewable sources need not be inverted. Along with electricity generated by the PV array and fuel cell, PVHYDRO also includes routines to simulate other domestic energy needs that include hot water and space heating. For hot water, a solar thermal system is included in the simulation to determine design parameters for a solar collector and hot water storage tank. PVHYDRO accomplishes space heating by a combination of methods including use of solar heated water, use of passive solar energy through windows, use of waste heat from the fuel cell, and combustion of a portion generated hydrogen via a catalytic burner. The catalytic burner also provides energy for domestic cooking by hydrogen combustion.

The starting point for the simulation to determine whether or not the system will be able to meet the load requirements is by reading in weather data contained in a file. The data can be supplied by the user, or TRNSYS provides typical meteorological year (TMY) data for 338 locations across the globe. This data includes average values for solar insolation, ambient temperature, and humidity.

As registered TRNSYS users we were able to request the source code for components found in the demonstration for our use and evaluation. Using a FORTRAN compiler, we were able to customize these non-standard components and link them with the main TRNSYS simulation program. Customization of the component models mainly involved refining their source code so that they accurately represent our electricity load profile and the performance of the specific equipment to be incorporated in our proposed IRHUS. At this stage of IRHUS development solar heating of water, residential heating, and catalytic combustion of hydrogen are excluded from the simulation.

7.4 Description of system components

7.4.1 Load Profile

Although different in magnitude, the load profile used to simulate the proposed IRHUS is similar to the one found in the PVHYDRO demonstration in that it represents typical residential electricity needs. In order to meet the requirements of the consumer load, the IRHUS must provide 58 kWh of AC electricity each day of the year, at 120 V and 60 Hz. The peak load each day is 10 kW, which occurs in the early evening, and the daily average load is 2.5 kW. The daily, peak, and average loads that the IRHUS system must supply also take into account losses encountered in AC/DC power inversion, DC/DC voltage conversion, and power requirements of various system components (i.e. controller).

Since the daily, peak, and average loads of the PVHYDRO demonstration differ from the IRHUS simulation, the component subroutines that simulate the electric consumers had to be customized to meet the needs of the IRHUS. Also, the size of various system components had to be adjusted in order to meet the increased capacity requirements of the IRHUS.

7.4.2 Batteries for Short Term Energy Storage

In the simulation of the IRHUS, batteries are included for short-term storage of electricity generated by the PV array and the fuel cell. Batteries play an important role for they supply the continuous demand of electricity required by the IRHUS. While holding a sufficient charge, they maintain a stable and constant flow of electricity to the electric consumer regardless of system interruptions involving the PV array or fuel cell. Such interruptions include lack of proper solar insulation, lack of hydrogen supply, and power "gaps" encountered when transferring electricity generation from the array to the fuel cell.

In the interest of keeping the IRHUS system as renewable as possible, it is desirable to include as few batteries as possible into the system design. Batteries tend to have a much shorter lifetime (5-10 years) compared to the renewable sources of electricity found in the system (20 years). However, as the amount of battery storage capacity decreases, the sizes of other system components, such as hydrogen storage capacity and size of the PV array, increase in order to compensate. In order to investigate this system trade-off, two simulation studies have been conducted on the proposed IRHUS.

Case 1 includes a total of four Exide brand lead-calcium deep cycle solar batteries. This brand of battery was chosen as a representative example of what may be used in a commercial system. The four batteries are connected in series which maintains a battery bus voltage of 48 V. The battery string has a capacity of 125 Ah, which permits the batteries to store 2 hours of required system amperage based on a daily consumption of 58 kWh. Case 1 represents a situation where the batteries are only able to supply the system load when electricity production switches between the PV array and the fuel cell. No means of safety back-up power is provided in the event that the PV array and fuel cell become inoperable.

Case 2 include a total of 12 batteries arranged in an array of three parallel strings of four batteries each. The same type of battery has been used in this simulation, however in this case each parallel string has a capacity of 635 Ah. With 1905 Ah total storage capacity, the battery array has the ability to solely power the load for 1.25 days, based on 58 kWh daily consumption, in the event system interruptions are encountered with the PV array or fuel cell. Also, in this case, the size of the battery array prevents the need for the fuel cell to be solely responsible for powering the load every evening, when the PV array is inactive. Instead, the fuel cell is only required to supply power when the battery state-of-charge drops below a certain "safe" limit, caused by consecutive days of low solar insolation. In a stand-alone PV system, batteries are usually expected to store between 3-7 days of useable power. Because a hybrid system has a secondary means of generating electricity, in this case a fuel cell, the number of days of storage required from the battery array can be significantly reduced.

7.4.3 Photovoltaic Array

In the IRHUS simulation, the PV array acts as the primary producer of electricity. It has been designed large enough to supply all electricity requirements based on average values of solar insolation. During prolonged periods when the insolation is lower than the average, the fuel cell is able to support the deficiency. During prolonged periods when the insolation is greater than the average, excess power generated by the array can be diverted to the electrolyzer, which effectively stores this excess energy by producing hydrogen, that can later be used by the fuel cell. Output from the weather data generator contained within the TRNSYS software supplies simulated values of solar insolation necessary to run the PV array model. For the IRHUS simulation, weather conditions in Orlando, FL have been chosen.

Siemens SR100 solar modules have been chosen as a representative example of modules that may be used in a commercial system. For case 1, a total of 588 individual modules are used in the simulation, and the array is configured with 147 parallel strings of 4 modules each. The panels are tilted at an angle of 45° to optimize electricity production during the winter months. Using the manufacturer's guaranteed power output of 100 W per module at standard test conditions (irradiance = 1000 W/m^2, cell temperature = 25 °C), the peak power output of the array is expected to be 58.8 kW.

For case 2, a total of 256 of the Siemens SR100 modules are used, and the array is configured with 64 parallel strings of 4 modules each. The panels are also tilted at an angle of 45°, and the peak output of the array at standard test conditions is expected to be 25.6 kW.

7.4.4 Electrolyzer

In the IRHUS system, the electrolyzer is coupled directly to the PV array and its primary function is to produce hydrogen during periods of above average solar insolation, or when all other load and battery requirements have been met. The TRNSYS subroutines for the electrolyzer have been modeled according to the performance of a Teledyne Altus alkaline electrolyzer.

For the IRHUS simulation, data for a Treadwell PEM type electrolyzer has been used in place of the Teledyne data that was provided along with the PVHYDRO demonstration. The IRHUS electrolyzer has a total of 25 cells and each cell is assumed to have an area of 279 cm^2. The electrolyzer operates at an efficiency of approximately 75%, producing approximately 0.48 kg/h (90 slpm) of hydrogen at 500 A.

7.4.5 Hydrogen Storage

A pressurized tank is included in the IRHUS simulation that stores hydrogen as it is produced by the electrolyzer. This arrangement allows a surplus of hydrogen to be available for use by the fuel cell even when no power is available to run the electrolyzer. The maximum pressure of the tank is 1000 psi. For case 1, an optimized storage volume of 20 m^3 is used in the IRHUS simulation, allowing a maximum of 90 kg of hydrogen to be stored at ambient (25 °C)

temperatures. For case 2, an optimized storage volume of 10 m^3 is used, allowing a maximum of 45 kg of hydrogen to be stored at 25 °C.

7.4.6 Fuel Cell

The IRHUS simulation includes a PEM fuel cell for secondary power generation. The TRNSYS subroutines for the fuel cell were created to model the performance of PEM type cells constructed at the Schatz Energy Research Center. For the IRHUS simulation available data for Energy Partners' new generation fuel cell stack has been entered in place of the Schatz data that was provided to us along with the PVHYDRO demonstration software.

The IRHUS fuel cell operates on hydrogen and air and contains a total of 50 cells. Each cell has an area of 300 cm^2. The stack produces a total of 11.6 kW of DC power at 32 V and 363 A. The stack operates at an efficiency of 44% consuming 0.683 kg/h (127 slpm) of hydrogen.

7.4.7 Power Conditioning

In the IRHUS simulation, four power conditioning devices are included (see Figure 7.1). A maximum power point tracker (MPPT) maintains optimum performance of the PV panels by ensuring that the array operates at the maximum power point on its I-V curve. A DC to DC converter upgrades the fuel cell output voltage to the battery bus voltage. A diode prevents the back flow of current from the battery array and fuel cell to the electrolyzer. This ensures that the only source of power for the electrolyzer is the PV array. Finally, a DC to AC inverter is included to invert the DC power supplied by the battery array to AC power required by the electric consumer. The efficiency of all power conditioning devices is assumed to be approximately 90%.

7.4.8 Controller

A single controller device oversees total system operation in the IRHUS simulation. By assessing the requirements and/or output available of every system component, including the electric load, the controller makes appropriate decisions to optimize system performance. These decisions include whether to connect or disconnect individual components to/from the system and whether power generated by the PV array is sent to the electrolyzer, for hydrogen generation, or to the battery array, for use by the electric consumer.

A generalized controller operational flowchart is included in Figure 7.2. This flowchart shows relative battery state-of-charge (SOC) to be the starting criteria for the decision tree. SOC is defined as the ratio of ampere-hours (Ah) stored in the battery array at any given time to the maximum Ah capacity of the array. During this process the actual controller subroutine also includes the voltage and current that is available and/or required by each component. However, for the purpose of explanation, the power available or required by various system components can be related to battery SOC.

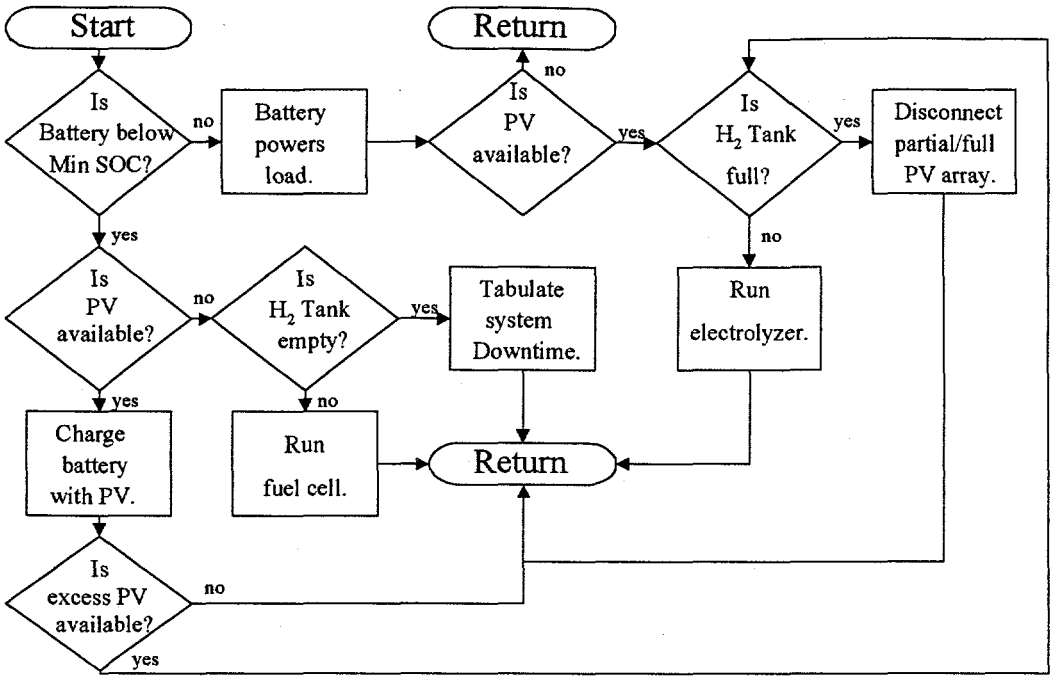

Figure 7.2: Controller Operational Flowchart

After determining whether battery SOC is below a certain minimum value, the controller can judge whether to use available power to charge the battery, or produce hydrogen. If the battery contains a sufficient charge, and PV power is available, hydrogen can be produced by the electrolyzer and stored. If both the battery and storage tank are full at any time, the PV array will power the load directly. This may involve either partially or fully disconnecting the PV array from the load, depending on the load requirements and the amount of solar insolation available. If the battery does not contain a sufficient charge, the controller will first try to charge the battery with the PV array. If excess power from the array is available, the controller will divert the excess power to the electrolyzer such that hydrogen can be produced in conjunction with battery charging. If insufficient solar insolation is available, the controller will then use the fuel cell to power the load, until the PV array permits the batteries to regain a sufficient state-of-charge. The only instance where system downtime can occur is when the system is exclusively relying on the fuel cell for power, and the hydrogen reserve is exhausted.

Summary of input variables for cases 1 and 2 are presented in Table 7.2.

Table 7.2 Input variables for simulation cases 1 and 2

	case 1	case 2
LOAD PROFILE		
AC Power Requirement	58.0 kW	58.0 kW
DC Power Requirement	0.0 kW	0.0 kW
Voltage	120 V	120 V
Amperage	83.3 A	83.3 A
BATTERY ARRAY		
Model	Exide Deep Cycle	Exide Deep Cycle
Type	lead-calcium	lead-calcium
Total Batteries	4	12
Series/Parallel	4S X 1P	4S X 3P
Cell Voltage	2.0 V	2.0 V
Cell Capacity	125 Ah	635 Ah
Array Voltage	48 V	48 V
Array Capacity	125 Ah	1905 Ah
Days of Storage	0.083 days	1.25 days
PHOTOVOLTAIC ARRAY		
Model	Siemens SR100	Siemens SR100
Type	single-crystal silicon	single-crystal silicon
Total Modules	588	256
Series/Parallel	4/147	4S X 64P
Module Voltage (Vmpp)	17.0 V	17.0 V
Module Amperage (Impp)	5.9 A	5.9 A
Module Power (Pmax)	100 W	100 W
Array Voltage (Vmpp)	68 V	68 V
Array Amperage (Impp)	867 A	378 A
Array Power (Pmax)	58.8kW	25.6kW
Array Tilt	45o	45o
ELECTROLYZER		
Model	Treadwell	Treadwell
Type	PEM	PEM
Number of Cells	25.0	25.0
Cell Area	279 cm2	279 cm2
Hydrogen Production	0.48 kg/h @ 500 A	0.48 kg/h @ 500 A
Efficiency	75%	75%
HYDROGEN STORAGE		
Type	Pressurized	Pressurized
Pressure	1000 psi	1000 psi
Volume	20 m3	10 m3
Maximum Storage Capacity	90 kg	45 kg
FUEL CELL		
Model	EP NG2000	EP NG2000
Type	PEM, H2/Air	PEM, H2/Air
Cell Voltage (Voc)	0.90 V	0.90 V
Cell Voltage (Vmpp)	0.520 V	0.520 V
Cell Amperage (Impp)	2000 mA/cm2	2000 mA/cm2
Cell Area	300 cm2	300 cm2
Number of Cells	50	50
Stack Voltage	32 V	32 V
Stack Amperage	363 A	363 A

Stack Power	11.6 kW	11.6 kW
Stack Efficiency	44.00%	44.00%
Hydrogen Consumption	0.683 kg/h	0.683 kg/h
POWER CONDITIONING DEVICE EFFICIENCY		
Max. Power Point Tracker	94%	94%
DC/DC Converter	90%	90%
Diode	90%	90%
AC/DC Inverter	90%	90%

7.5 Simulation results

Figures 7.3.1a and 7.3.1b show system performance of case 1 for the first week of February and August respectively. In these plots the power produced by the PV array is shown along with the power requirement of the system load and battery SOC. Figures 7.3.2a and 7.3.2b show system performance for the first week of February and August, respectively, for case 2.

Examples of controller operation are shown in Figures 7.4.1a and 7.4.1b for case 1 and Figures 7.4.2a and 7.4.2b for case 2, for the first week of February and August respectively. These figures show how the controller decides when to operate the electrolyzer and fuel cell, based on the battery SOC. The plots for both the electrolyzer and fuel cell represent their on/off condition, where a 0 value corresponds to "off" and a value of 1 corresponds to "on". In these plots instances where the fuel cell is not operating at full capacity can be seen. This characteristic is a result of how the controller subroutine was originally created. In the PVHYDRO demonstration there is a water and space heating requirement along with the electric load. The demonstration relies on the fuel cell to generate a portion of this heat during operation. In order to maximize fuel cell heat production, when the battery contains a sufficient state-of-charge (i.e. the fuel cell is not needed for power generation) but the heating load is large, a small fraction of the total number of individual fuel cells will be activated such that heat can be generated.

Figures 7.5.1a and 7.5.1b show examples of how the system produces, stores, and uses hydrogen for case 1. Figures 7.5.2a and 7.5.2b show this data for case 2. These plots are also for the first week of February and August, respectively. Each plot shows the power drawn by the electrolyzer, and how the amount of hydrogen produced affects the value for hydrogen storage. As with battery SOC, hydrogen storage is represented as the ratio of the amount of hydrogen in the tank at any time to the maximum capacity of the tank. The plots also show the power produced by the fuel cell, and how the amount of hydrogen consumed affects the amount of hydrogen reserve.

Figure 7.6.1 shows simulation results for battery SOC and hydrogen storage over the course of an entire year for case 1, starting at the beginning of January and terminating at the end of December. Figure 7.6.2 shows this result for case 2. As can be seen in these plots, battery SOC fluctuates daily between a relatively constant minimum and maximum value. Values for hydrogen storage fluctuate seasonally with a minimum value occurring in February and a maximum value occurring in August.

7.6 Discussion

Along with the design of each individual IRHUS component, total system operation plays a major role in system performance, size, and cost. Each of the individual components are intimately linked together in some way, therefore changing the size or operational parameters of one component has the potential to disturb the balance of the entire system. Simulations of the proposed IRHUS have been conducted with the intent of optimizing system performance, rather than cost, however it is expected that an optimized system will also be the most cost effective. The primary parameter that is intended to be the basis for optimization is the value for hydrogen storage. Other mandatory system criteria included use of a PEM type fuel cell and electrolyzer, maximizing battery lifetime, and maintaining zero percent system downtime.

As seen in Figure 7.6.1 and 7.6.2, over the course of the year the controller allows the battery array state-of-charge to fluctuate between its maximum value, which corresponds to 3500 Ah, to 50% of its maximum value. The extra and essentially "unused" storage capacity has been included in the design for two reasons. First, it provides a small amount of backup power in the event of primary (PV array) and secondary (fuel cell) electricity producer interruptions. Second, maintaining a low level of acceptable battery discharge (50%) significantly extends the expected life of the battery array.

Depending on what time of year the start-up of the IRHUS system occurs, the hydrogen tank should be initially charged with the amount of hydrogen found in Figures 7.6.1 or 7.6.2 that corresponds to that particular time of year. The optimized storage tank values of maximum pressure and storage volume ensure that the tank is never completely empty, and rarely completely full to account for expected variation in weather conditions. Starting up the IRHUS with a different value than what is found in Figure 7.6.1 or 7.6.2 will perturb this balance. Starting with more hydrogen than necessary will not cause system downtime, however the system will be overdesigned and will not utilize the full potential of each system component. Starting with less hydrogen than depicted will eventually cause system downtime during the winter season.

The criteria used by the controller to decide when to operate the fuel cell and electrolyzer has also been optimized. Running the electrolyzer slightly before the battery array has reached its maximum state-of-charge effectively lowers the PV power requirement, thereby reducing the size of the array. Controller settings for how often the fuel cell operates are also important operational parameters. Since the fuel cell represents mainly a capital expense, it is desirable to use it to generate power as often as possible, rather than just during the winter. Therefore the PV array is tilted at an angle of 45° which optimizes winter time performance of the panels, when there is less solar insolation available, according to the sun's winter time position in the sky. This arrangement also requires use of the fuel cell during the summer months, rather than leaving an expensive piece of equipment to lye dormant for several months. The controller can also be programmed to operate the fuel cell more often than in the current simulations to put less of a demand on the PV array for power production, however, the size of the array would actually increase to supply the increased hydrogen demand. Under this condition, the size of the storage tank would also increase.

As seen by the results of simulations for case 1 and case 2, a system trade-off exists among battery array storage capacity, hydrogen tank storage capacity, and the size of the PV array. With a smaller battery array, less energy can be stored in this short-term medium, and therefore the size of the hydrogen tank must increase in order to store enough energy for use when the PV array is inactive. Because hydrogen production is initiated by the electricity produced by the PV array, the size of the PV array must increase in order to support day-time electricity production as well as the increased hydrogen demand.

It is possible that other forms of hydrogen storage besides the pressurized storage investigated in the current simulation (i.e. metal hydride) will lower the cost of the storage component. However the relative amount of hydrogen necessary will essentially remain the same. Since the intent of this simulation was to optimize system performance, investigating feasibility of other forms of hydrogen storage has been left until the costing phase of the project takes place.

It is also possible that storing oxygen produced by the electrolyzer for use in the fuel cell rather than ambient air will lower the overall cost of the system. Since the only thing that varies when including oxygen storage is the efficiency, and therefore cost, of the fuel cell, this feasibility study has been left for the costing phase of the project. During this phase, the reduced fuel cell cost can be weighed against added cost of adding oxygen storage.

7.7 Conclusion

After conducting a search for applicable simulation software, TRNSYS was chosen as a viable platform for performing simulations on the proposed IRHUS. The simulation code was customized in order to model the specific characteristics of proposed system components. A realistic load profile was chosen as an example application for the renewable energy produced by the IRHUS system, and system components have been designed and optimized to meet this load with zero percent system downtime. Results from simulations of two cases, one with four batteries and one with twelve batteries, show that a system with fewer batteries and therefore more renewable requires a larger PV array to supply necessary power, and may therefore be more costly. This analysis, along with to potential to store oxygen produced by the electrolyzer and the use of metal hydrides to store hydrogen, has been left for a later stage of the project, where a detailed cost analysis can be conducted.

7.8 References

1. C. Gregoire Padro, V. Putche, M. Fairlie, *Proc. XII World Hydrogen Energy Conference, Buenos Aires, Argentina,* 1998, 2247
2. J. Vanhanen, P. Lund, *Int. J. Hydrogen Energy,* v.20, 575, 1995
3. H. Barthels, W. Brocke, K. Bonhoff, et al. *Int. J. Hydrogen Energy,* v.23, 295, 1998
4. P. Lehman, C. Chamberlin, *Int. J. Hydrogen Energy,* v.16, 349, 199
5. S. Galli, G. De Paoli, A. Ciancia, , *Proc. X World Hydrogen Energy Conference, Cocoa Beach, Florida, USA,* 1994, 439

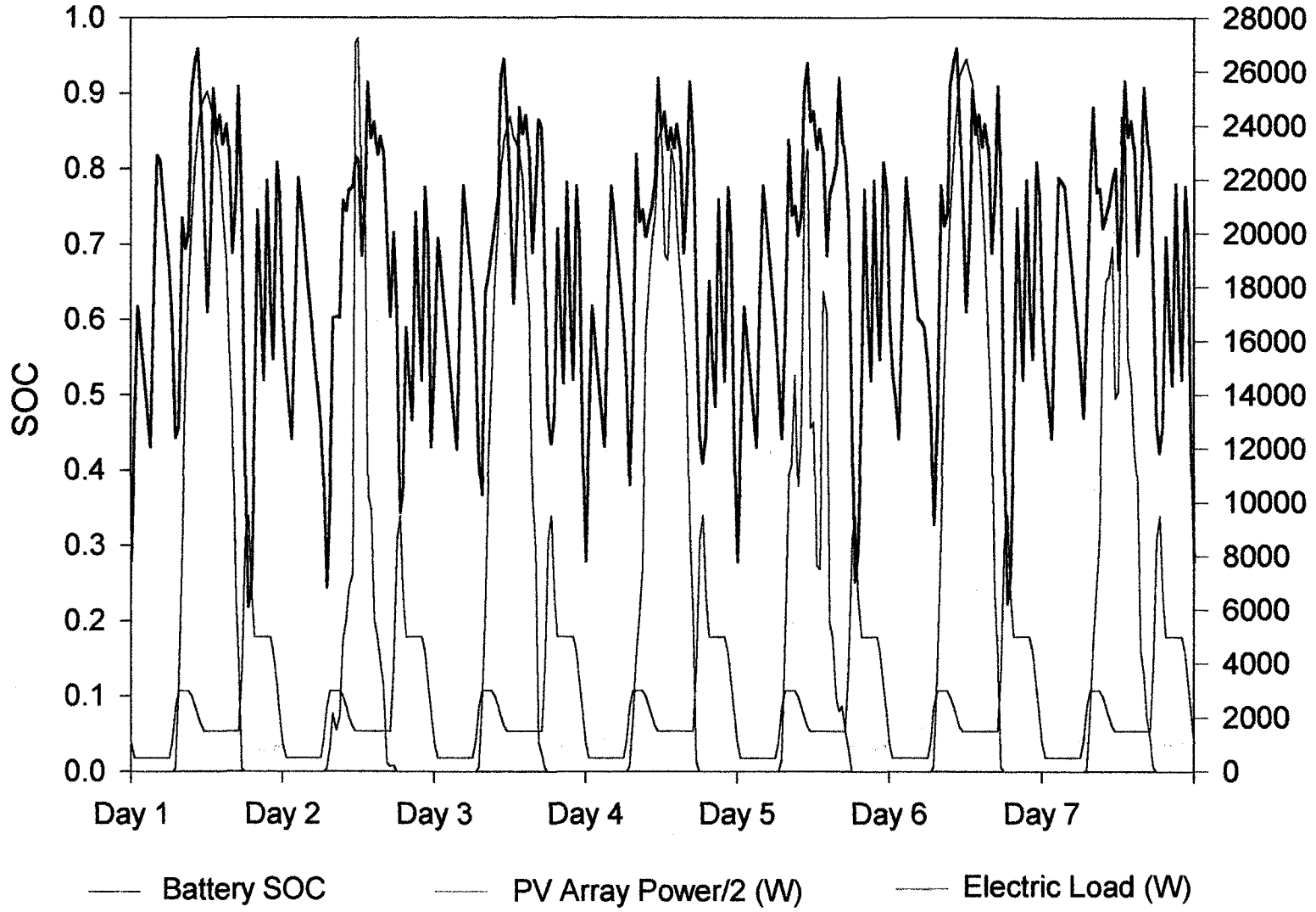

Figure 7.3.1a February, Week 1

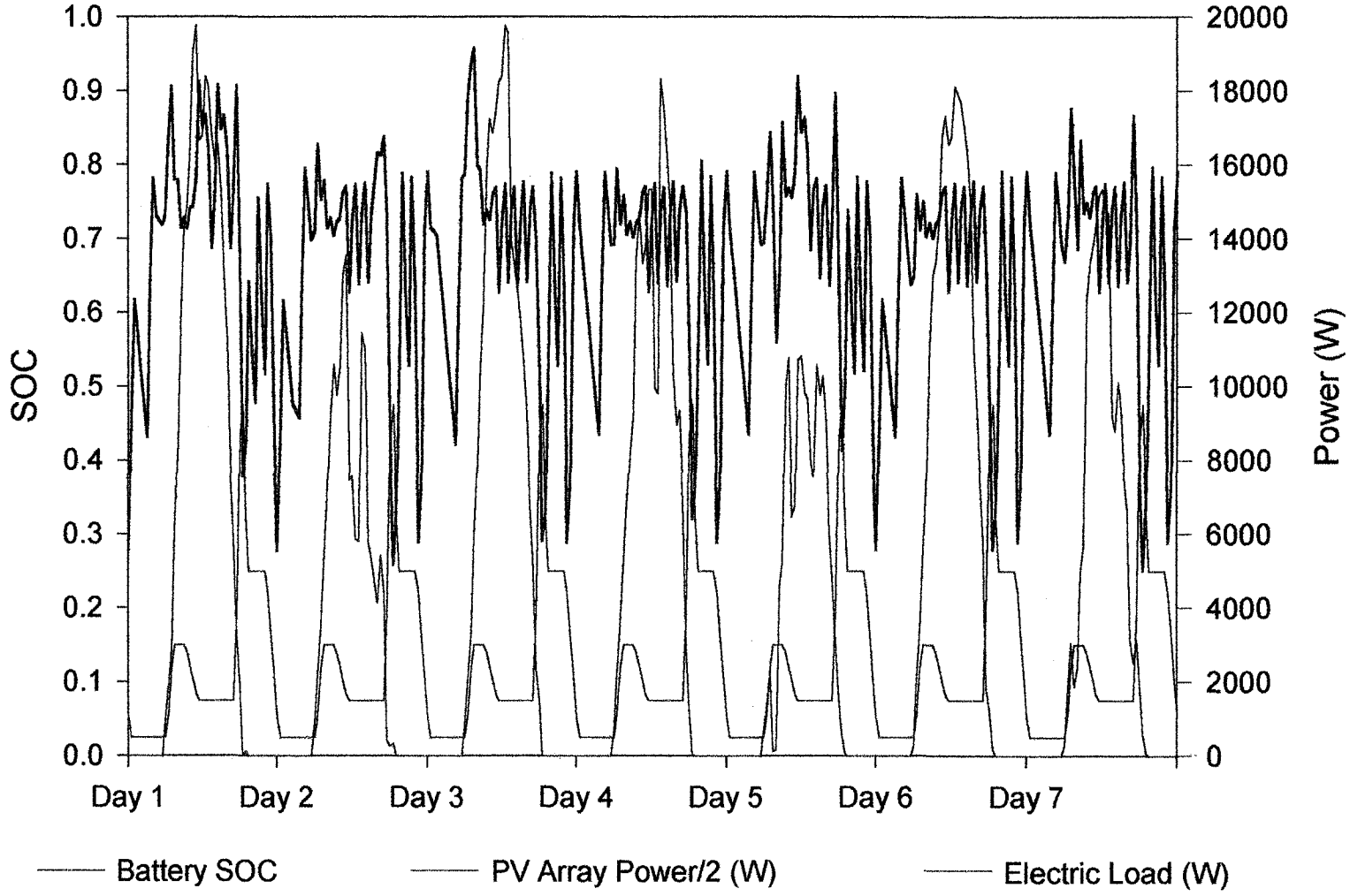

Figure 7.3.1b August, Week 1

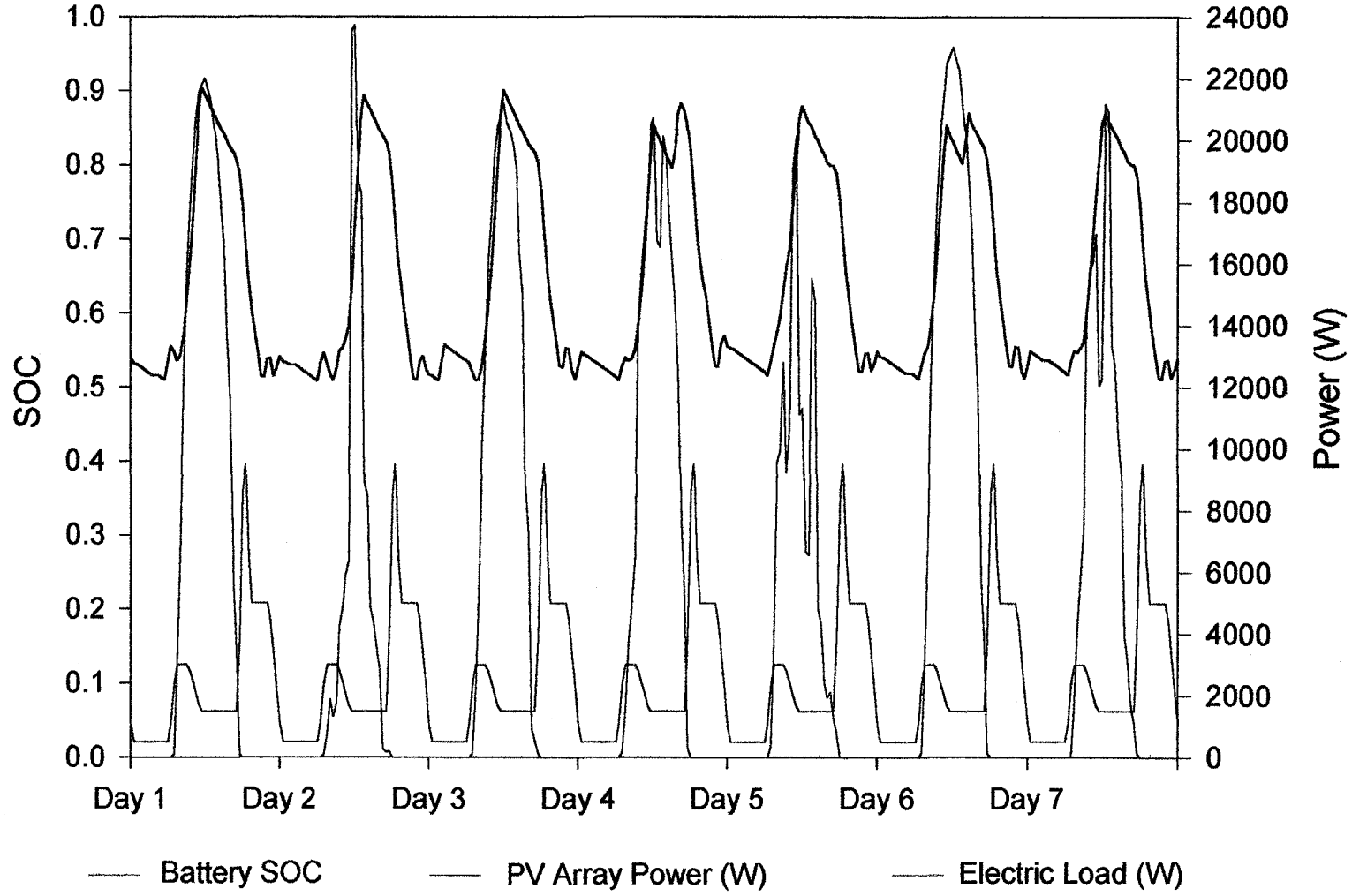

Figure 7.3.2a February, Week 1

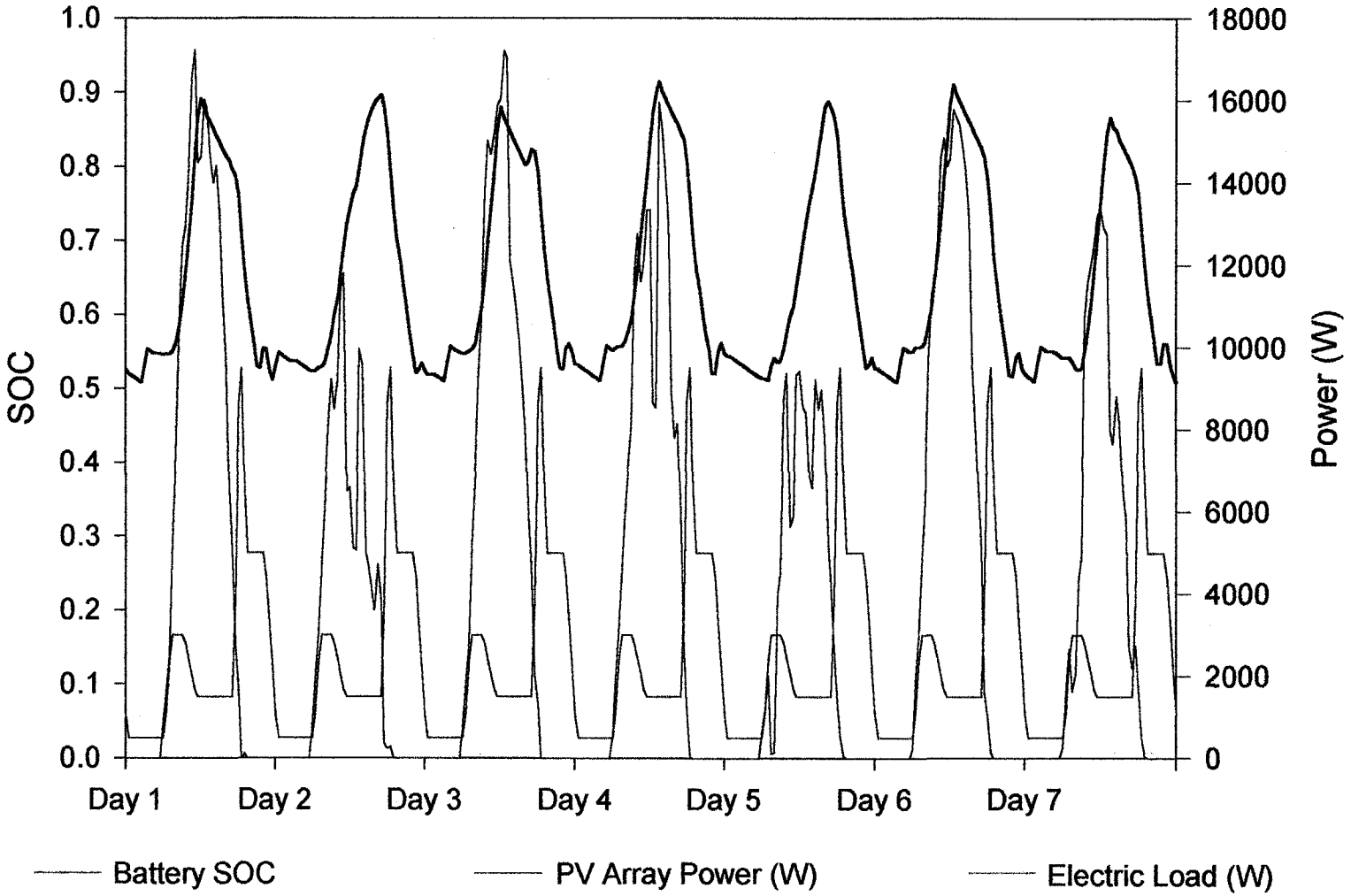

Figure 7.3.2b August, Week 1

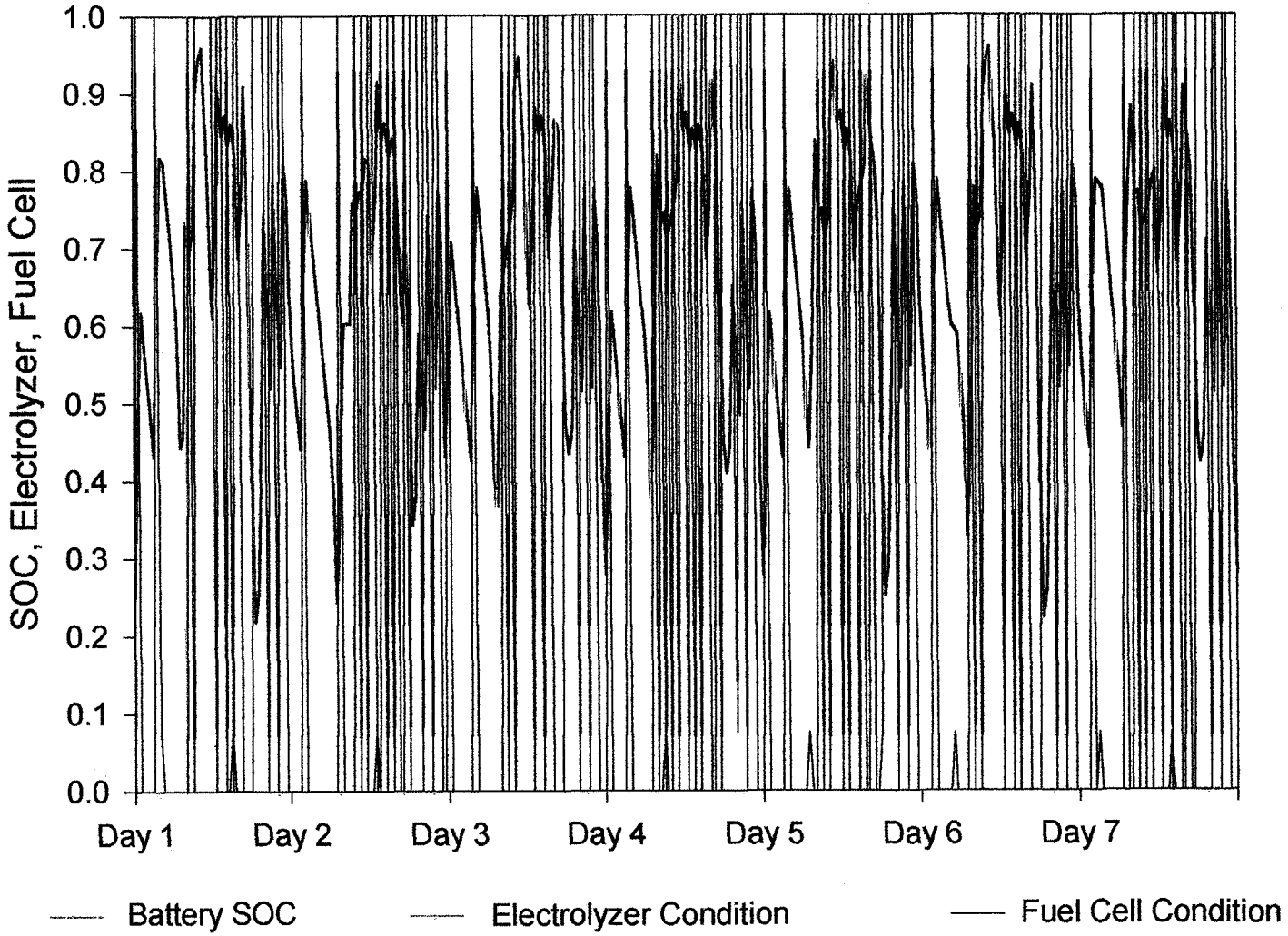

Figure 7.4.1a February, Week 1

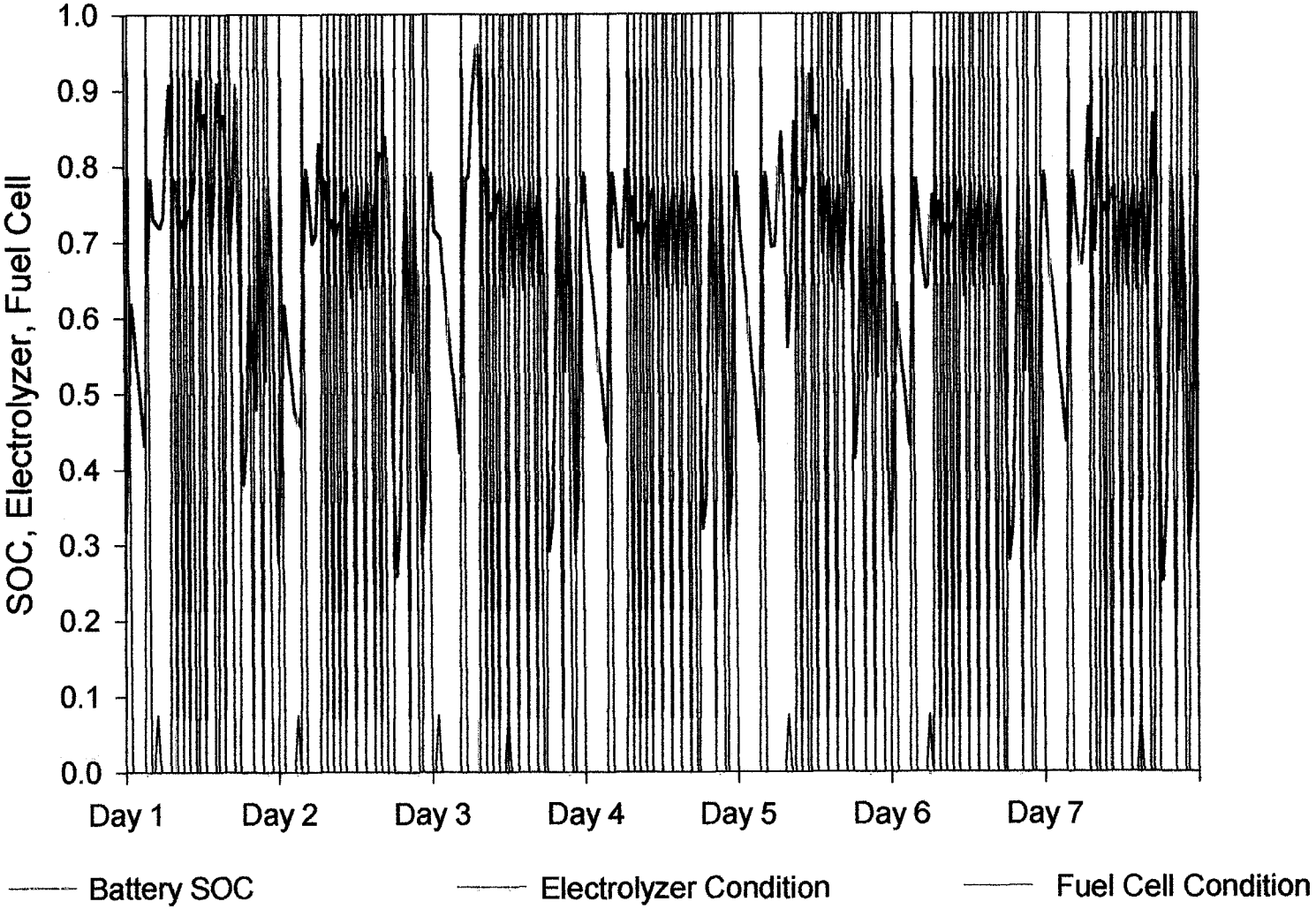

Figure 7.4.1b August, Week 1

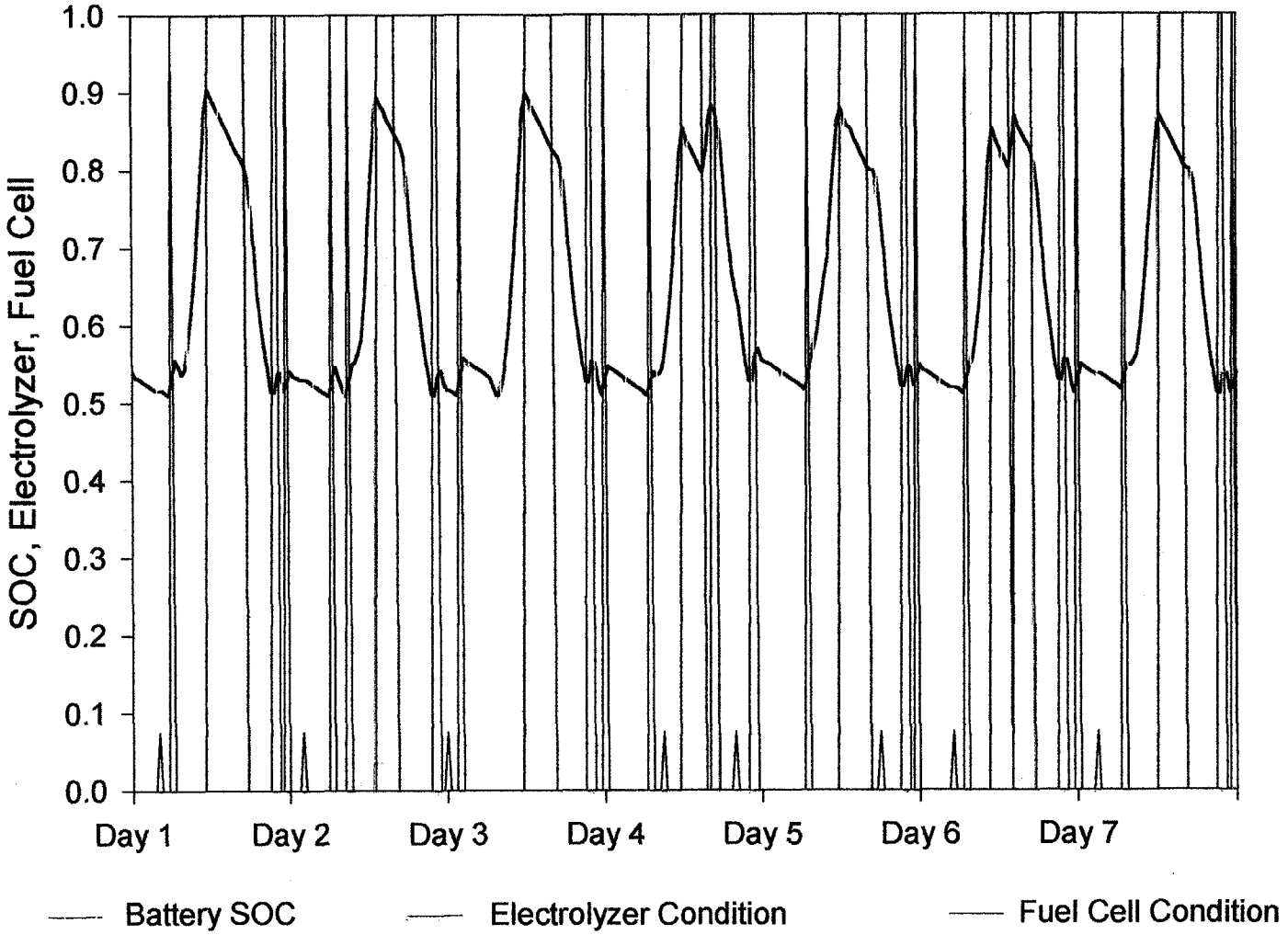

Figure 7.4.2a February, Week 1

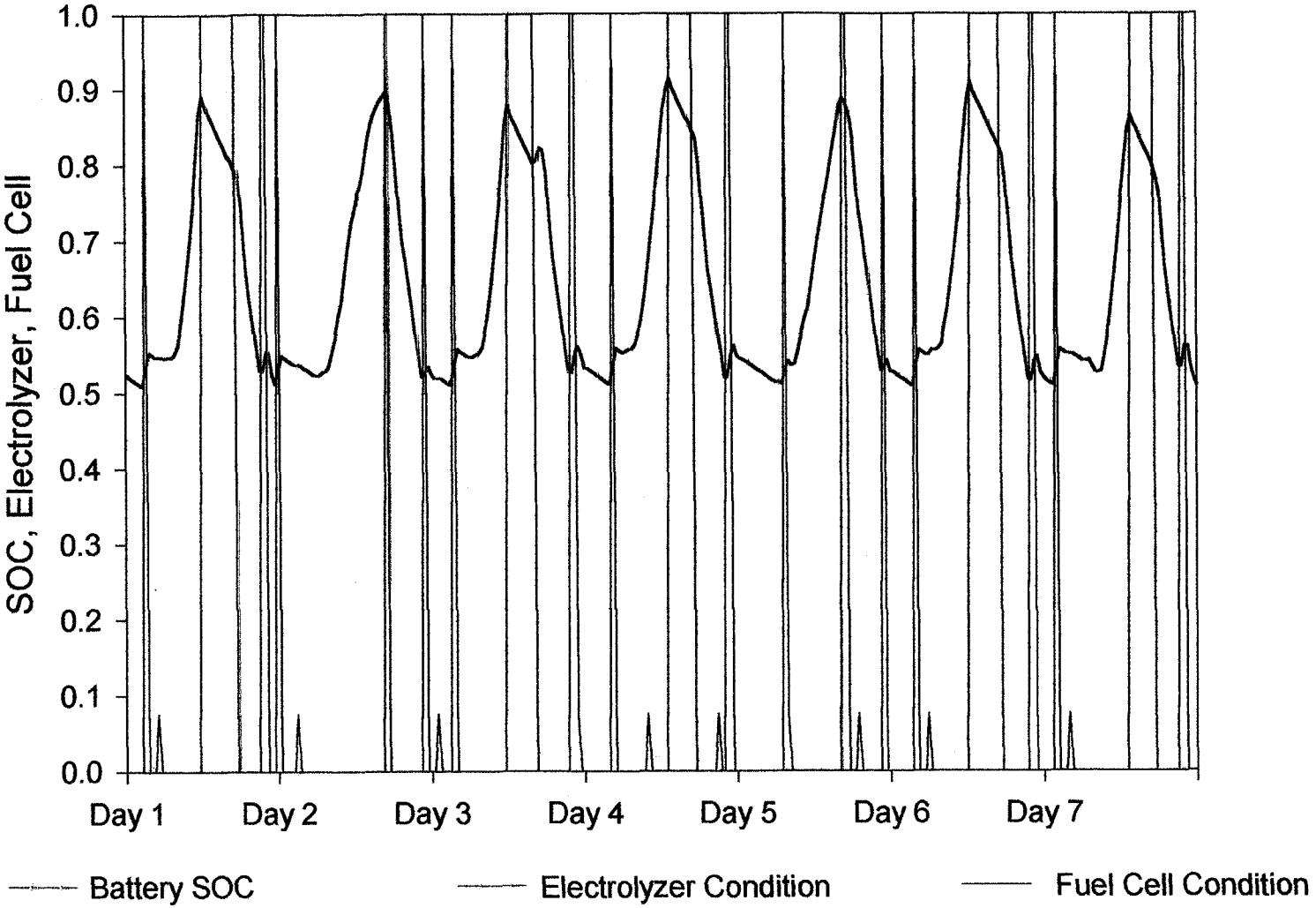

Figure 7.4.2b August, Week 1

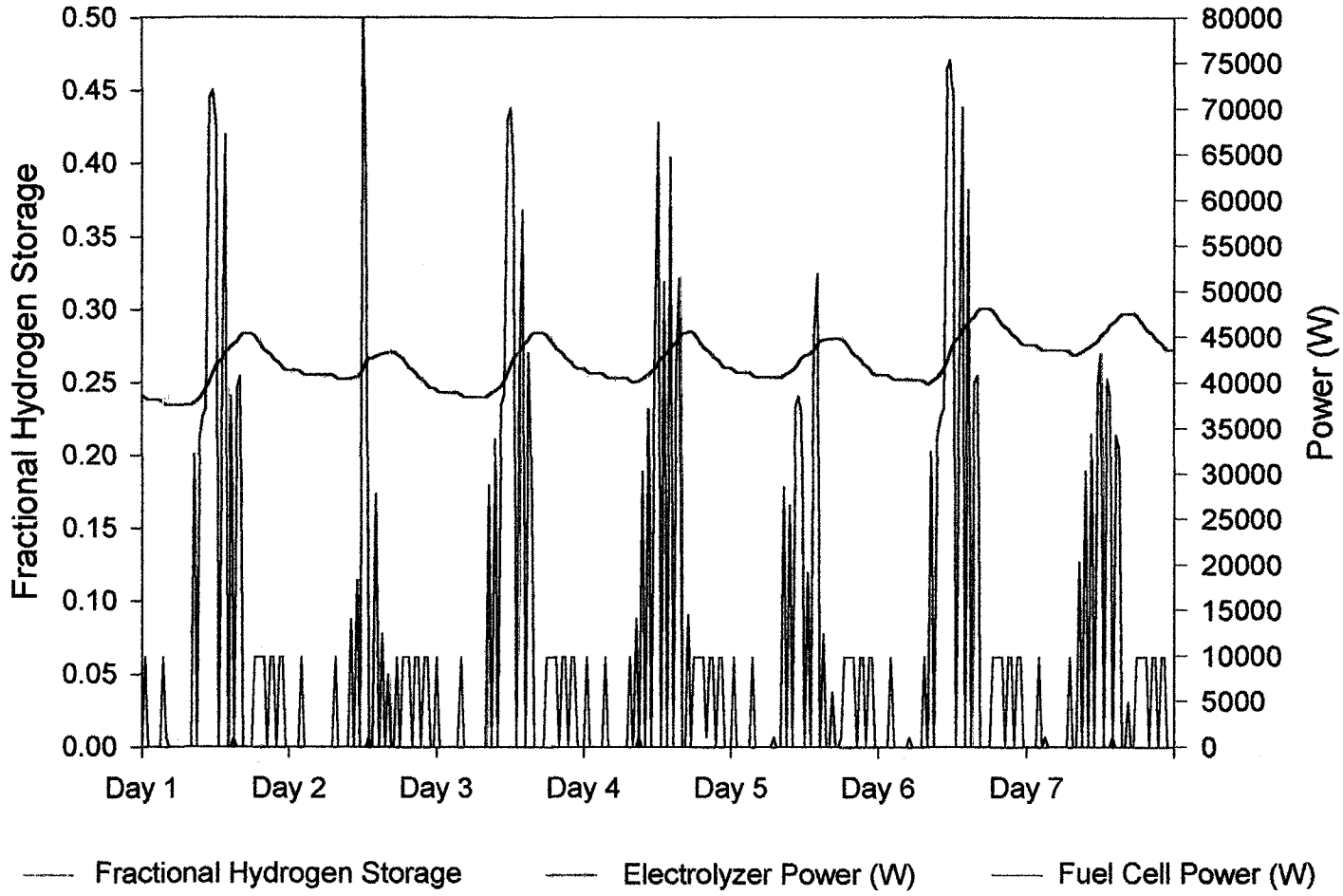

Figure 7.5.1a February, Week 1

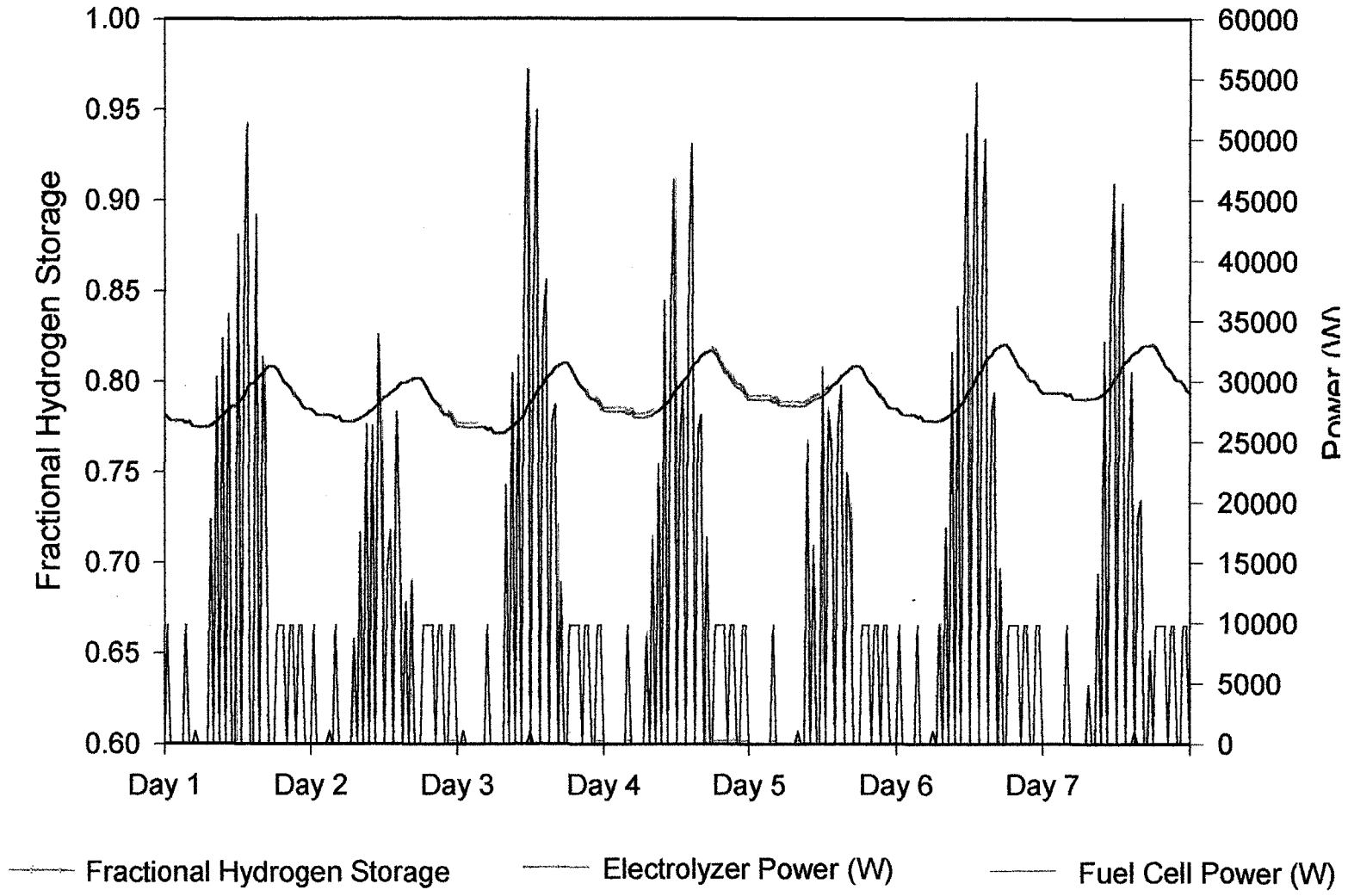

Figure 7.5.1b August, Week 1

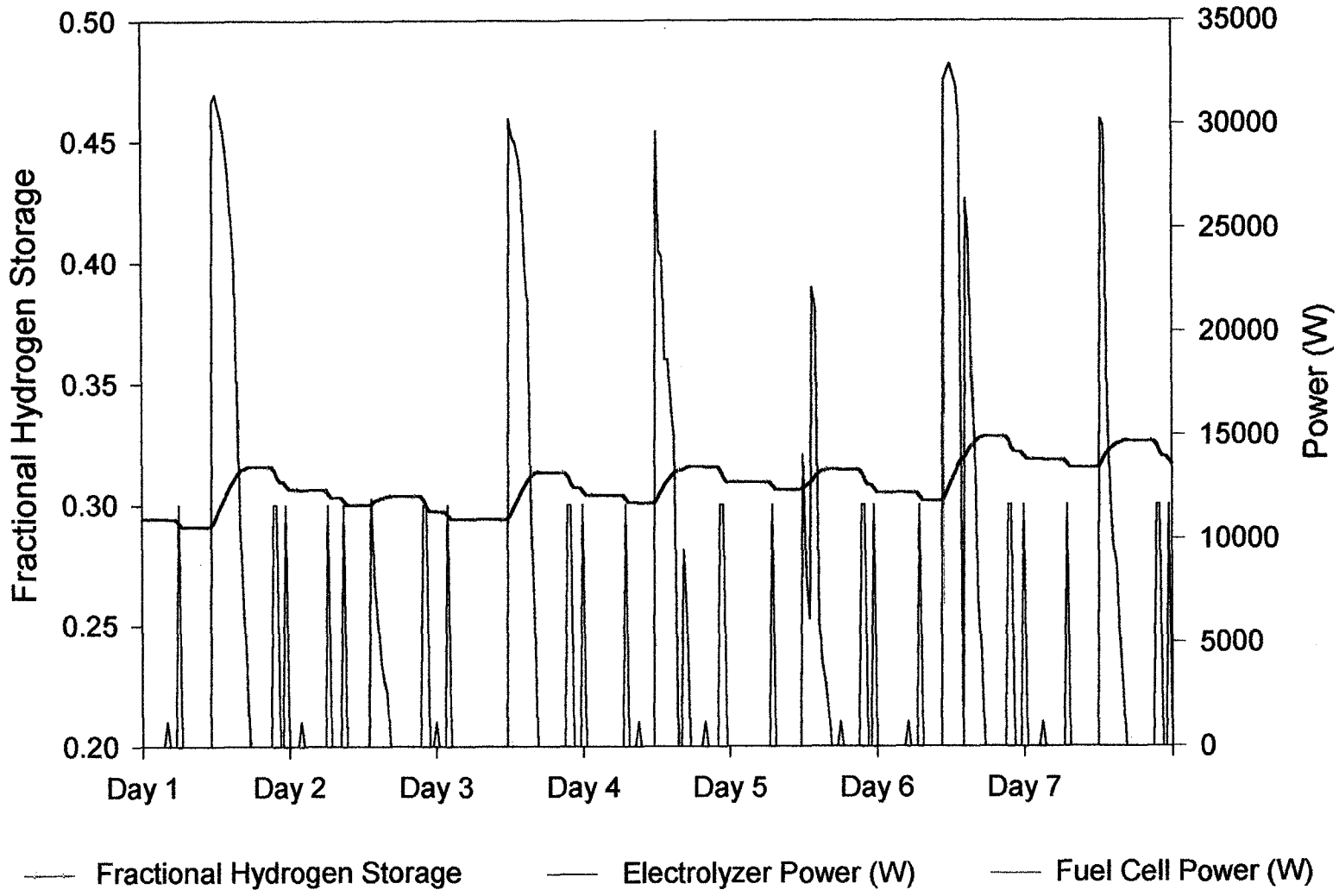

Figure 7.5.2a February, Week 1

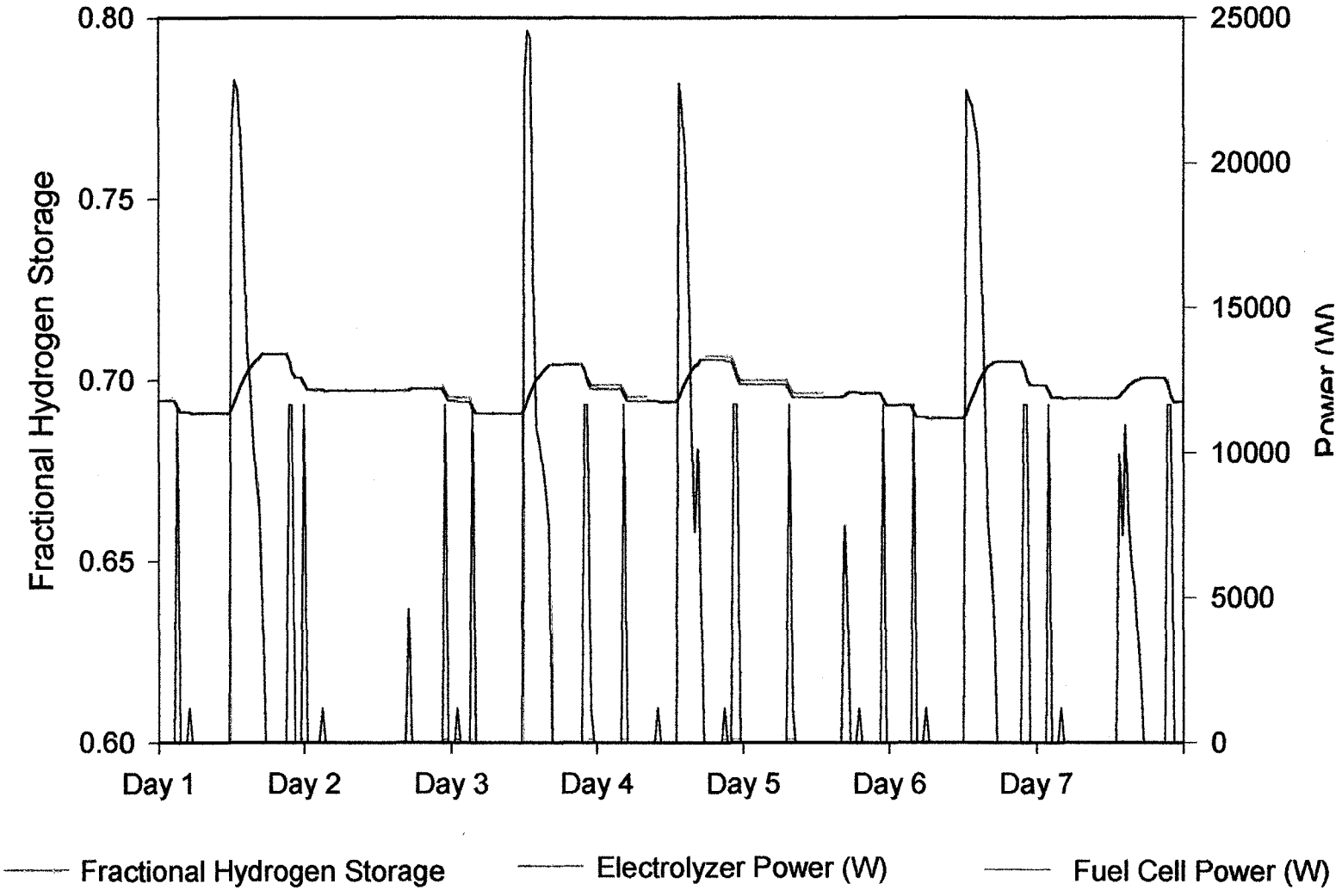

Figure 7.5.2b August, Week 1

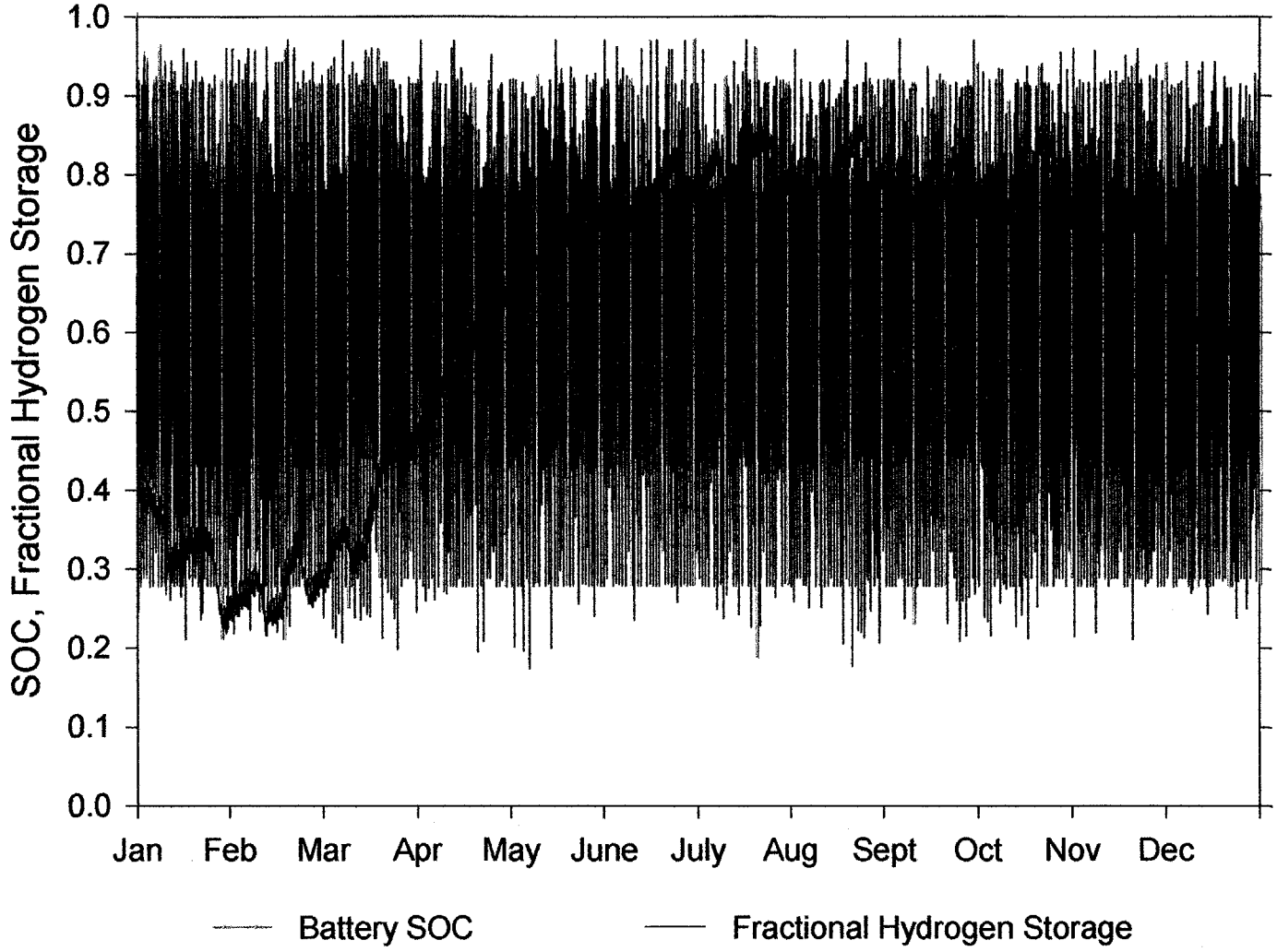

Figure 7.6.1 Yearly Performance

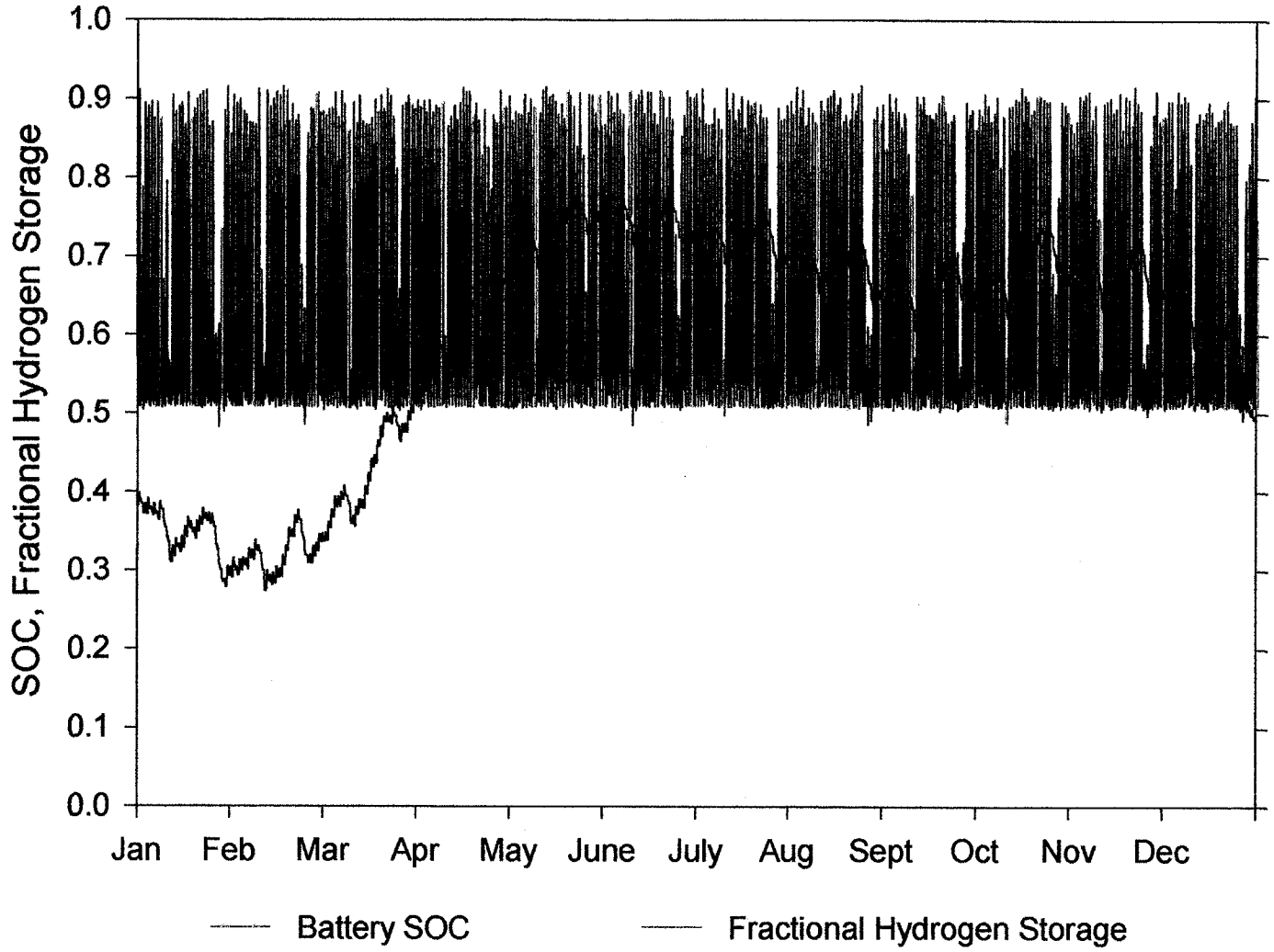

Figure 7.6.2 Yearly Performance

8. Conclusions from Phase I and Recommendations

Based on the results of the analyses presented above the following conclusions may be reached:

- The integrated renewable hydrogen utility system is technically feasible. It delivers power to the users when it is needed. As an extra bonus (which was not included in the above analysis), both hydrogen and oxygen that are generated in the process may have commercial use and value (hydrogen as a transportation fuel and oxygen for water treatment, in hospitals or in research facilities).
- Power supply in remote areas and on isolated islands has been identified as a potential market, with three different power levels 1 kW, 10, kW and up to 100 kW.
- The system does not make any impact on the environment – it generates no emissions and it generates no noise. As such it may be used for power supply in environmentally sensitive areas, such as national parks.
- The round-trip efficiency (electrolyzer and fuel cell) is about ~40%. This relatively low efficiency makes it difficult to compete with other methods of energy storage, such as batteries, particularly for short term storage.
- The cost of electricity out can be several times higher than the cost of electricity in because of low round-trip efficiency, low capacity factors and relatively high capital costs. This limits application to the cases that can justify high cost of around-the-clock electricity availability.
- The electrolyzer power is several times higher than the fuel cell power. This is related to the renewable source availability and the system inefficiency.
- The electrolyzer has a very low capacity factor (about 22%), which has a significant impact on the cost of electricity. Commercial usage of hydrogen (and potentially oxygen) may increase the electrolyzer's capacity factor and improve the system's economics. (The cost of hydrogen refueling station must then also be taken into account).
- An air fuel cell would be at least twice as big as oxygen fuel cell. An oxygen fuel cell is more efficient (up to 75% at partial load). A detailed cost analysis is required that would take into account the capital cost of the fuel cell and blower on one side and oxygen storage and oxygen recirculation pump on the other side, as well as the efficiencies of the systems to be compared. Safety of oxygen storage must also be taken into account.
- The lowest electricity cost results with a high fuel cell operating voltage, which requires a large but efficient fuel cell stack.
- The lowest electricity cost results with a high electrolyzer voltage, thus less efficient but more compact electrolyzer stack. This is due to electrolyzer's high capital cost and low capacity factor.
- The automotive market may bring down the cost of fuel cells because of mass-production. Unfortunately, no such market may be envisioned for the electrolyzer, which implies that the cost of the electrolyzer would remain to be a problem, particularly having in mind heavy Pt catalyst loading and extensive use of expensive materials, such as Nb and Zr.

- TRNSYS appears to be a viable tool for system simulation. The simulation results provide insight on system performance under various conditions, however more precise simulation under realistic conditions and loads is required.

- In order to alleviate the problem of high electrolyzer capital cost and low capacity factor, it definitively makes sense to investigate the possibility of a reversible fuel cell, i.e., combine the functions of fuel cell and electrolyzer in a single unit. Based on preliminary analyses, it seems that there is a good match between the electrolyzer and fuel cell size (in terms of active area, current density and number of cells). However, developing such a device on a multi-kilowatt level is not an easy task and it is out of the scope of this project. Energy Partners may consider including a reversible fuel cell in its development plans, if funding is available. Some adjustments in Energy Partners' business plan would be necessary in order to allocate the resources.

9. Plan for Phase II

Task 1 System design

Based on the results of the first phase, both technical and business part, we will design the system as a commercial product. Early in Phase II a decision would have to be made on the system's configuration (oxygen vs. air). The emphasis in this phase will be on details and packaging. The system will be designed as a stand-alone unit, with electrical and water connections, and control panel at the outside. Particular attention will be devoted to safety issues (such as selection of materials, locations of vents, etc.), as well as to selection of materials for enclosure (since the system will be intended for use in remote and island locations where it typically will be exposed to severe atmospheric conditions). In the design process we will use standard engineering tools and design packages such as AutoCAD and SolidWorks. As an example, Figures 9.1 – 9.3 show an envisioned hydrogen fueled fuel cell power system.

Task 2 Components development

The following components were identified to need some development or at least modification of the existing:

- Fuel cell and the fuel cell supporting system:
  - If a H_2/O_2 fuel cell is selected only minor changes would be required on Energy Partners exisiting fuel cell stacks. Energy Partners has expertise (and the patents) on H_2/O_2 fuel cell systems.
  - If air operation is selected, the stack and the system would require some development efforts and design changes in order to efficiently operate at low pressure. Although Energy Partners state-of-the-art fuel cell stacks can operate at low pressure, they and the supporting system are not optimized for low pressure operation. The issues are primarily on water and thermal management.
  - The most difficult path would be development of a regenerative fuel cell (unitized electrolyzer/fuel cell). Development of such a device is not in the scope of this project. Energy Partners may consider including a reversible fuel cell in its development plans, if funding is available.

- The electrolyzer may also need some design changes. This work is currently being performed by Treadwell, but under another government funded project, but Treadwell has agreed to contribute such an electrolyzer to this project.
- A custom made controller/power conditioning unit will be needed. This work will be performed at Trace Engineering.

Task 3 Prototype development

For verification of system design and components' modifications, we will design, build, test and demonstrate a pre-production prototype. Power output level of this prototype will be carefully determined according to the following criteria:

- allow selection of standardized "off-the-shelf" equipment,
- match selected existing renewable energy component's power output,
- not too large in order to keep the cost within a budget,
- not too small in order to have meaningful and practical demonstration.

For the purpose of completing the cost estimates we assumed that a 2-10 kW prototype would be developed and demonstrated in Phase II. The exact nominal power output will be dictated by the available electrolyzer (Treadwell does not intend to build a custom electrolyzer for this project but use one of the electrolyzers developed in another project), and available renewable source (photovoltaic array) for testing.

The team members will acquire necessary parts and fabricate the main components, in accordance with previously defined component specifications and their standard manufacturing practices. Each component will be tested at manufacturer's site. All the components and parts will be delivered to Energy Partners, and the prototype will be assembled in Energy Partners facilities.

A control strategy will be selected to match the available renewable energy power source for demonstration. Upon completion of the system, the system will be subjected to vigorous functional testing to verify proper functioning of the components and the system, and to establish performance specifications.

Task 4 Demonstration

Once the system functional tests are completed, the system will be delivered and installed at the demonstration site, Florida Solar Energy Center (FSEC), where it will be connected to an existing renewable energy power source – a photovoltaic array already installed at FSEC. The work in this task will include installation, monitoring, data acquisition and maintenance, both emergency and scheduled. FSEC has extensive experience testing and monitoring systems performance. The center has operated monitoring systems to automatically collect and archive monitored data from on site and remote systems for more than 15 years. FSEC currently collects more than 500,000 data points daily from a large variety of field monitoring experiments being conducted across the nation - from Oregon to New York to Florida.

One of the EP vehicles (Genesis or John Deere Gator) will be delivered to the demonstration site and refueled to demonstrate the system's versatility and capability to generate hydrogen fuel.

The goal of this demonstration phase is not only to demonstrate the components' and system's operational capabilities, operational reliability and longevity, but also to fine tune the design and particularly to develop and validate the control strategy.

Task 5 Demonstration on the island

As an ultimate demonstration at the end of the program the system will be installed at Lee Stocking Island, Bahamas, where it will be used to provide power for the Caribbean Marine Research Center facilities. There already exists a PV-array on the island with an aging battery bank. The system will be used to replace the battery bank. If necessary, the PV array will be refurbished and/or expanded. The system will be equipped with remote monitoring and control capabilities.

Task 6 Plans for manufacturing

In parallel with demonstration we will summarize the results of Phase I and Phase II and make plans for manufacturing of the system as a commercial product. Some utility companies (such as Trust Power from New Zealand) and potential users (such as National Tropical Botanical Gardens in Hawaii) have already expressed interest in systems similar to the one being developed in this program. The manufacturing plan will include analysis of volumes, materials, processes, equipment, personnel and capital required to manufacture the system as a commercial product.

Task 7 Testing of the market strategy and refinement of the business plan

Refinement of the business plan will continue in Phase II with particular emphasis on: cost estimate for start-up manufacturing plan, market research and analyses, identifying targets for the skimming strategy of pricing, investigation of the status of similar efforts by competitors, economic study and strategy for government subsidies, development of a warranty plan, and development of a contingency plan for raising capital in a timely manner. At the end the business and marketing plan will be revised considering the information generated above. This work will be performed by the Perry Foundation in cooperation with the Applied Business Research Institute of the Rinker School of Business, Palm Beach Atlantic College.

Schedule

The work in Phase II will proceed in accordance with the following schedule:

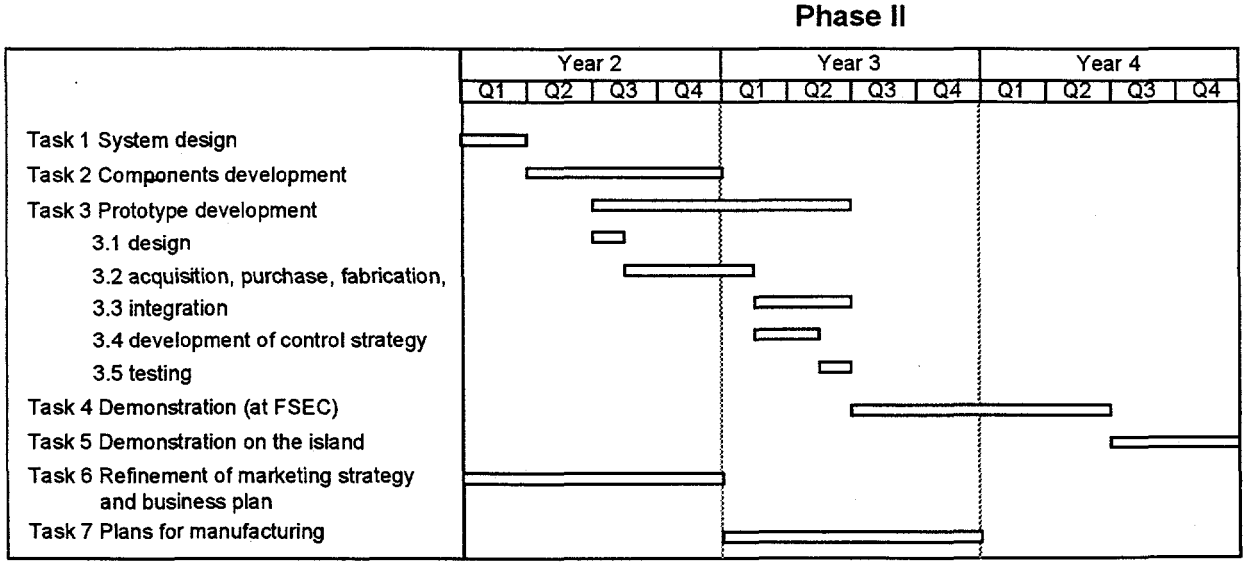

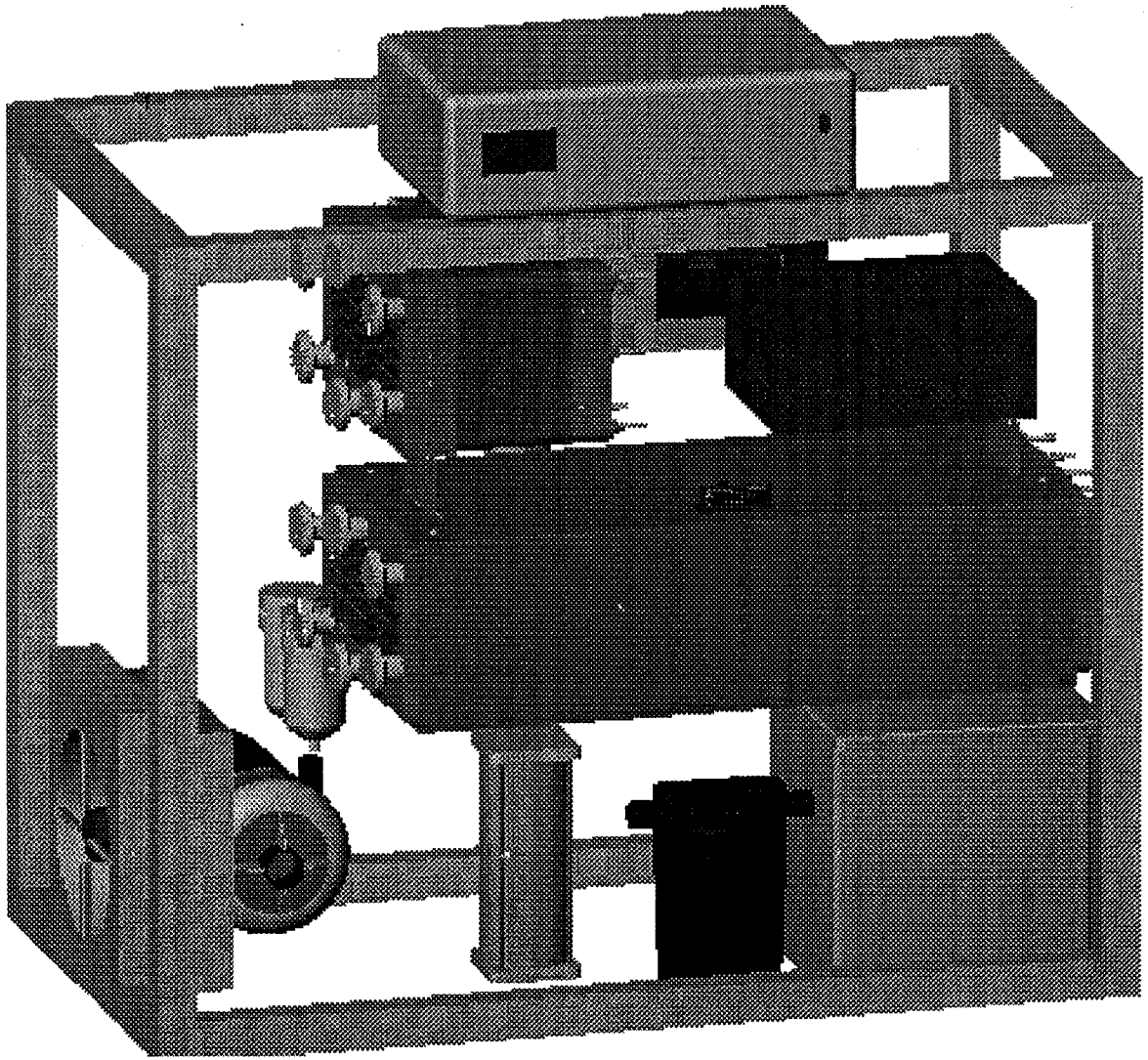

Figure 9.1 Conceptual design of a hydrogen fuel cell power system – front view

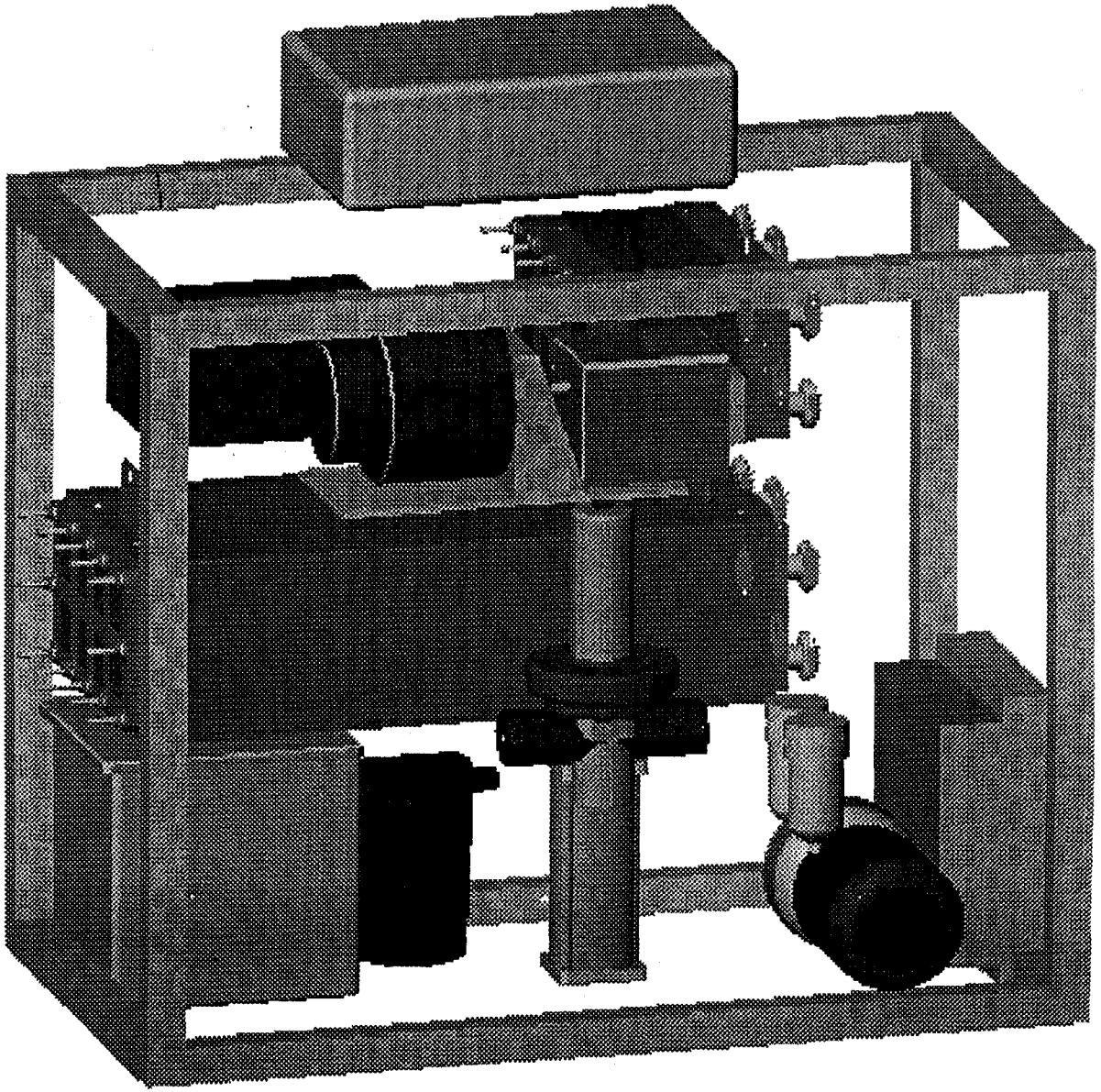

Figure 9.2 Conceptual design of a hydrogen fuel cell power system – back view

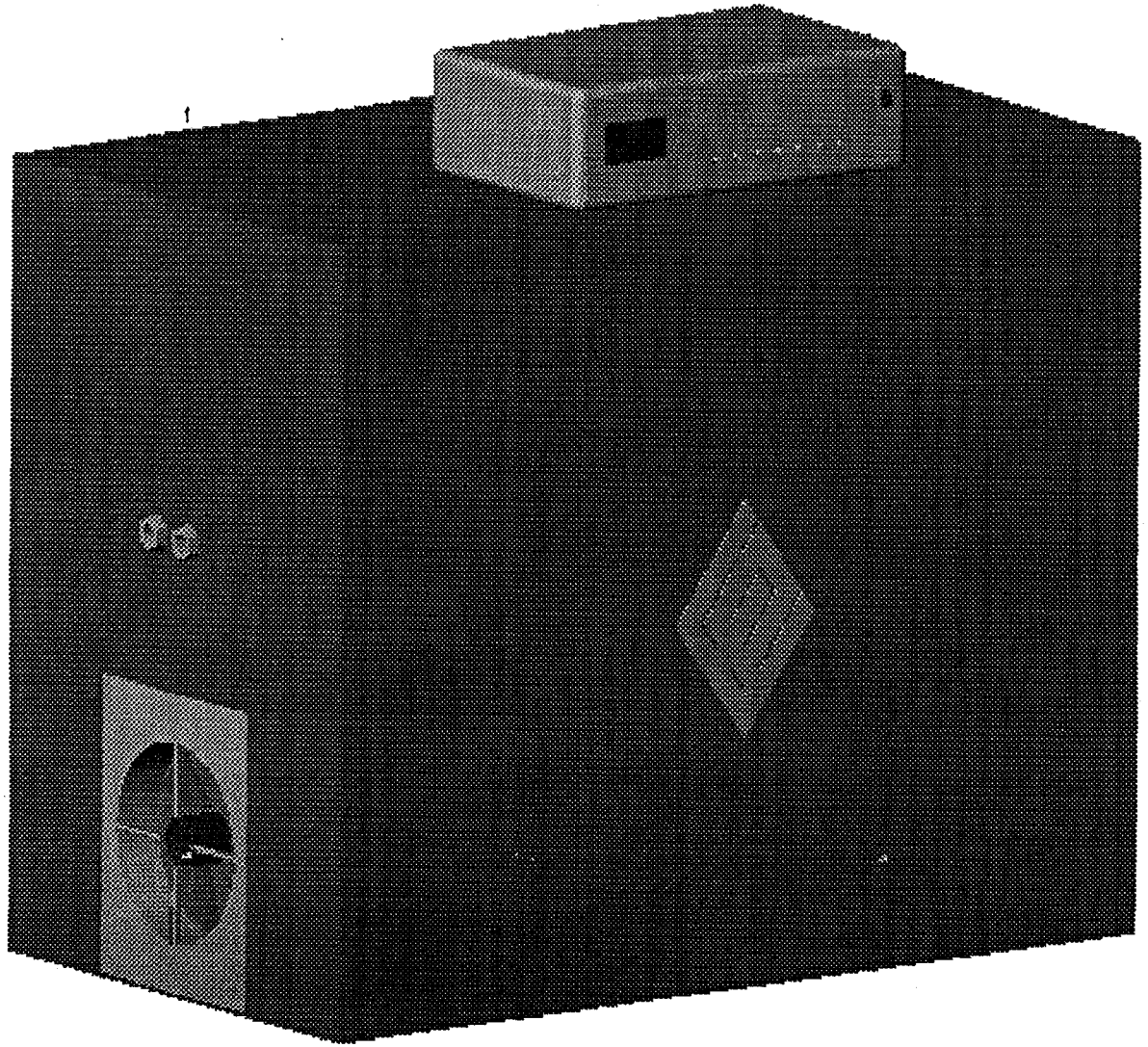

Figure 9.3 Conceptual design of a hydrogen fuel cell power system – with cover